

Advancing **Practical guidelines for reproducible N₂O flux chamber measurement techniques measurements in nutrient-poor ecosystems**

Nathalie Ylenia Triches ^{1,2}, Jan Engel ¹, Abdullah Bolek ¹, Timo Vesala ³, Maija E. Marushchak ⁴, Anna-Maria Virkkala ⁵, Martin Heimann ¹, and Mathias Göckede ¹

¹Department of Biogeochemical Signals, Max Planck Institute for Biogeochemistry, Jena, Germany

²Institute for Atmospheric and Earth System Research/Forest Sciences, Faculty of Agriculture and Forestry, University of Helsinki, Helsinki, Finland

³Institute for Atmospheric and Earth System Research/Physics, Faculty of Science, University of Helsinki, Helsinki, Finland

⁴Department of Environmental and Biological Sciences, Faculty of Science, Forestry and Technology, University of Eastern Finland, Kuopio, Finland

⁵Woodwell Climate Research Center, Falmouth, USA

Correspondence: Nathalie Ylenia Triches (ntriches@bgc-jena.mpg.de)

Abstract. Nitrous The atmospheric concentration of nitrous oxide (N₂O) is the third most important greenhouse gas whose atmospheric mole fraction has risen from 273 ppb to 336 ppb has increased significantly since 1800, mainly due to agricultural activities. However, due to their large area, nutrient-poor natural soils, including those in the (sub-) Arctic, also emit and consume play a crucial role in N₂O . These have not been investigated thoroughly, partly because of emissions and consumption. Despite their importance, these soils have been understudied due to methodological limitations in reliably detecting low fluxes. These limitations were, to a large extent, driven by the available instrumentation: lacking portable gas analysers for with appropriate accuracy, researchers relied on manual air sampling from closed flux chambers, with subsequent analysis using gas chromatographs (GC) in a laboratory. In this study, we use a Our study addresses this knowledge gap by testing a fast-responding, portable gas analyser (PGA; Aeris MIRA Ultra N₂O/CO₂) combined with a custom manual chamber system, incorporating both transparent (light) and opaque (dark) measurements, for its suitability to measure low manual chambers (height and diameter: 25 cm) for measuring N₂O fluxes from a nutrient-poor, sub-Arctic peatland. We assess the performance of the analyser under low-flux conditions, evaluate the effects of chamber closure time, and compare linear and non-linear models for quantifying concentration gradients. Moreover, we compare flux rates based on high-frequency *in situ* observations against an approach that randomly draws discrete samples from the full time series, mimicking a GC-based approach. Our results show that with our PGA, we can successfully detect and calculate this setup can detect and quantify low N₂O flux rates, with a mean of $12.9 \pm 28.4 \text{ nmol m}^{-2} \text{ h}^{-1}$ under light conditions and $-46.1 \pm 38.2 \text{ nmol m}^{-2} \text{ h}^{-1}$ under dark conditions, depending on chamber closure time. The majority of fluxes (88% for light and 74% for dark measurements) and standard error of $-0.61 \pm 0.08 \mu\text{g N}_2\text{O-N m}^{-2} \text{ h}^{-1}$ for a 5-min closure time, as observed in our study. More than 70% of the measured N₂O fluxes exceeded the minimum detectable flux ($\text{MDF } 0.027 \pm 0.0002, \mu\text{mol m}^{-2} \text{ h}^{-1}$), which was $14.5 \pm 1.05 \text{ nmol m}^{-2} \text{ h}^{-1}$ for light and $14.7 \pm 1.08 \text{ nmol m}^{-2} \text{ h}^{-1}$ for dark measurements. Our comparison of chamber closure times (3–10 min) showed that 3 minutes may be insufficient for capturing varied according to chamber closure time. Our study highlights the importance of using fast-responding analysers to measure low N₂O fluxes during light measurements, while closure times of 4–10 minutes provide more reliable results. For dark measurements, where and improve our understanding of diverse N₂O uptake was highest with short closure times, flux dynamics. For nutrient-poor soils, we recommend a chamber closure time of 3–approximately 5 minutes, unless data are limited, in which case longer times may help capture fluxes above the MDF. In our study, all fluxes were calculated using the . We also found that a non-linear model or matched the linear model when data showed a linear distribution. Compared to

the PGA-based flux calculations, GC-simulations underestimated fluxes when using 3-6 samples. Therefore, we suggest that flux calculation model yielded better results and was broadly applicable, including cases where data were linearly distributed. Overall, our study demonstrates the potential of fast-responding analysers may be better suited to measure low to improve our understanding of N₂O fluxes and improve the understanding of diverse flux dynamics in nutrient-poor soils.

1 Introduction

Nitrous oxide (N₂O) is the third most important greenhouse gas (GHG) with a global warming potential almost 300 times stronger than carbon dioxide (CO₂) over a period of 100 years (IPCC, 2023). It stays in the atmosphere for around 110 years and acts as an ozone-depleting compound in the stratosphere, causing direct harm to humans (IPCC, 2023). The atmospheric mole fractions of have , and its atmospheric concentration has increased from 273 ppb to 336 ppb since 1800 (Thoning et al., 2022). As most of this increase can be attributed to human activities, particularly the use of nitrogen (N) fertilisers in agriculture, research has focused on N₂O emissions from managed, agricultural soils (De Klein et al., 2020) that hold the potential for high N₂O emissions. This is because the input of nitrogen fertilisers in managed soils N increases the readily available mineral N needed for plant growth and thus increases harvest, but, simultaneously, can also result in higher N₂O emissions (Myhre et al., 2013).

Until about 15 years ago, only few studies investigated N₂O fluxes in the (subsub-) Arctic, where soils often have a very low availability of reactive N (Virkkala et al., 2024) and thus are not expected to emit or take up amounts of N₂O relevant for the global climate (Voigt et al., 2020; Christensen et al., 1999; Grogan et al., 2004). (Voigt et al., 2020; Christensen et al., 1999; Grogan et al., 2004; Martikainen et al., 1993). In these low N ecosystems, N₂O uptake could be expected, but has, so far, not been confirmed in field studies (Buchen et al., 2019; Schlesinger, 2013). Since 2009, multiple studies have reported N₂O emissions similar to agricultural soils from organic-rich ecosystems in the Arctic (Repo et al., 2009; Marushchak et al., 2011; Elberling et al., 2010), shifting the focus to only selected, high-nutrient areas within the (sub) Arctic. Nevertheless, reporting near-zero N₂O fluxes is crucial to avoid overestimating emissions caused by biased site selection favoring favouring high-emitting areas (Voigt et al., 2020).

In most studies, N₂O concentrations were sampled repeatedly with a syringe from the head space of a closed flux chamber and measured with a gas chromatograph (GC) in the laboratory (Hensen et al., 2013; Denmead, 2008; Pavelka et al., 2018). With this approach, typically between 4 and 9 6 discrete air samples are taken to measure the trend in N₂O mixing ratios during chamber closure time and calculate the fluxes. The sensitivity of GCs varies, but with only 4-9 few samples drawn from a fluctuating time series that may not necessarily display a linear trend, differences in low concentrations are hard to capture and highly dependent on single data points (Hübschmann, 2015). Additionally, in previous studies, opaque chambers have been mostly used because temperature inside the chamber would increase less above the ambient temperature compared to transparent chambers (Clough et al., 2020). As a result, there are only few studies investigating N₂O fluxes under different light conditions (Stewart et al., 2012). Since this was the only available method for *in situ* N₂O measurements in the field, our knowledge on (subsub-) Arctic N₂O fluxes is rather limited and makes it challenging to establish accurate baseline estimates, which are essential for detecting changes in fluxes.

Recent advances in laser spectroscopy led to novel, portable (< 15 kg) and fast-responding (1 Hz, *i.e.*, sampling every second) GHG analysers, offering new possibilities to measure low N₂O concentrations in nutrient-poor ecosystems (Subke et al., 2021). These portable gas analysers (PGAs) allow near-continuous monitoring of concentration changes, providing higher precision and lower detection limits than GC-based methods (Hensen et al., 2013). While differences in flux estimates between PGA and GC PGAs and GCs have been well-documented for CH₄ and CO₂, few studies have focused on N₂O (Christiansen et al., 2015; Brümmer et al., 2017). At the same time, many of the The detection limit was a significant constraint, as many reported N₂O fluxes were found to be below the detection limit, making it challenging to assess the magnitudes and possible uptake of these fluxes. It is crucial to know at which accuracy fluxes can be measured, and how to best measure them.

below the threshold of the GC method, limiting the ability to accurately assess their magnitude and trends. The availability of portable gas analysers PGAs for *in situ* N₂O flux measurements raises new methodological questions. First, in contrast to and , where chamber closure time of Unlike CH₄ and CO₂, where, under a fixed chamber height, approximately 3 min or less is minutes are well-accepted , it remains unclear how long chambers need to be closed for reliable for reliable measurement, the minimal chamber closure time for N₂O flux measurements fluxes flux in nutrient-poor ecosystems is unclear. This is due to the low concentrations of because N₂O , which need more time than and concentrations are very low and take longer to accumulate in the chamber head space in order to reach a sufficiently high change in concentration to detect a significant trend over the instrument noise and to reliably calculate the fluxes head space to accurately detect trends (Fiedler et al., 2022). Few studies have investigated the chamber closure time with portable N₂O analysers, and the reported recommendations range between 3 and 10 min (Fiedler et al., 2022; Brümmer et al., 2017). Second, there is a long-ongoing discussion within the chamber community on whether to use and originate from ecosystems with higher N₂O flux rates (Fiedler et al., 2022; Brümmer et al., 2017).

The chamber community has been discussing the use of linear (LM) or non-linear (HM) models to calculate flux rates (Kutzbach et al., 2007), which has not been investigated for low fluxes for decades (Pumpanen et al., 2004). The critique on the linear models is that they underestimate the flux rates due to the assumption that GHG concentrations keep increasing within the chamber head space (Fiedler et al., 2022) (Fiedler et al., 2022; Hüppi et al., 2018). However, it is clear from the theory of molecular diffusion that the rate of concentration change within the chamber declines over time (Hutchinson and Mosier, 1981; Kutzbach et al., 2007; Kroon et al., 2008), which then leads to the underestimation of fluxes when using linear models (Hüppi et al., 2018). As a result of that, there have been great efforts to implement non-linear flux calculations as alternatives for to LM, for example, through software packages (Pedersen et al., 2010; Hüppi et al., 2018). Nevertheless, the use of However, non-linear flux calculations is still not a standard within are not commonly used in the chamber community, most likely due to its complexity. likely because they are more complex to implement. For N₂O, there is a lack of data sets from nutrient-poor ecosystems to evaluate the effect of LM and HM models.

The main aim of this paper is to provide a first, extensive data set of present a mobile flux chamber method capable of quantifying (very) low N₂O fluxes measured with our measurement system consisting of a in nutrient-poor ecosystems. Using a novel portable N₂O analyser and both transparent and dark flux chambersto quantify (Aeris MIRA Ultra N₂O/CO₂) and our custom-made transparent and opaque flux chambers, we provide the first extensive data set of low N₂O in a nutrient-poor ecosystemfluxes from the (sub-) Arctic. We tested the instrument performance of our PGA in the laboratory and in the field , with our data set covering across various land cover types from a thawing permafrost peatland in sub-Arctic Sweden. We compare compared N₂O flux rates across calculated from different chamber closure times (3 min- 10 min) and evaluate evaluated differences between linear and non-linear calculation

methods. Moreover, we compare **Additionally, we compared** flux rates based on high-frequency *in situ* observations against an approach that randomly draws discrete **samples data points** from the full time series, mimicking a GC-based approach. Finally, we aim to provide guidance on measuring N₂O fluxes in nutrient-poor ecosystems, such as the Arctic. Ideally, this will encourage researchers to measure low fluxes in **sub-Arctic (sub-) Arctic** regions, get a better process understanding of N₂O fluxes, and
95 determine how the N cycle in nutrient-poor ecosystems will **react to global respond to Arctic** warming.

2 Methods

To facilitate the reader's understanding, we use the terminology proposed by Fiedler et al. (2022), with location describing the area where sampling occurs ("Stordalen mire"), site describing a vegetation unit within the location ("palsa lichen", "palsa moss", "bog", "fen"), and chamber base position (*i.e.*, plot) for the exact spot where N₂O was measured. With "chamber closure
100 time", we specify the time frame a chamber was closed onto the soil; one of these periods is then called "measurement period".

2.1 Study location and sampling sites

All data were collected at the Stordalen mire, a complex palsa mire underlain by sporadic permafrost located in subarctic Sweden (68° **200 20.0'** N, 19° **300 30.0'** E), 10 km east of Abisko (Ábeskovvu in Northern Sámi language). Permafrost has been rapidly thawing at this location over the last decades, and only remains in the dry uplifted areas on the peatland (palsas)
105 (Sjögersten et al., 2023). For our study, we randomly selected 24 chamber base positions in three transects on a dry-to-wet thawing gradient from palsa to bog to fen, with 6 replicates for each land cover type: palsa lichen, palsa moss, bog, and fen (Fig. 1). Transects 1 and 2 each contain 6 chamber base positions and are located in the northern **center centre** of the mire, within the footprint of an Integrated Carbon Observation System (ICOS, SE-Sto) eddy covariance tower which has been operating since 2014 (Lundin et al., 2024), Fig. 1). Transect 3 lies in the most north-eastern part of the palsa.

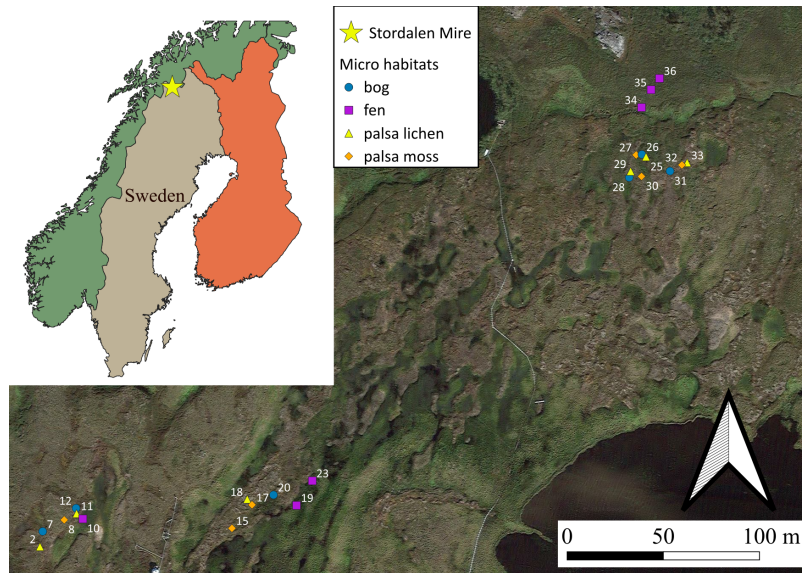


Figure 1. Three transects with chamber base positions in Stordalen (overlaid on satellite image from ©Google Maps). The location of the Stordalen Mire (the shape files of each country can be found at , last access: 17/09/2024) mire is marked with a star. Here, each micro habitats are represented with different colours colours and symbols for clarity. The spatial data of each country can be found at <https://simplemaps.com>, last access: 17/09/2024)

110 Vegetation on the palsa is mainly dominated by lichen (*Cladonia spp.*), shrubs (*Empetrum hermaphroditum*, *Betula nana*, *Vaccinium uliginosum*, *Vaccinium vitis-idaea*, *Rubus chamaemorus*) and some mosses (*Dicranum elongatum*, *Sphagnum fuscum*). Both bogs and fens contain peat-forming mosses (*Sphagnum balticum*, *Sphagnum lindbergii*, *Sphagnum riparium*), with the dominant vascular plants on fens being cotton grass (*Eriophorum vaginatum*, *Eriophorum angustifolium*) and in bogs sedges (*Carex rotundata*, *Carex rostrata*). The soils in the area are classified as organic histosols or, if permafrost occurs within
115 2 m of cryoturbation activities, as cryosols (Siewert, 2018). Research at the Stordalen mire has been conducted for over a century (Jonasson et al., 2012; Callaghan et al., 2013), and a vast amount of data on CH₄ and CO₂ fluxes has been published (Łakomiec et al., 2021; Varner et al., 2022). The mean annual temperature at the Stordalen mire is -0.6°C and the annual precipitation 304 mm (Malmer et al., 2005).

The data presented in this study were collected during three separate campaigns covering different seasons: spring (between
120 23 - 30 May 2023), summer (20 - 27 July 2023), and autumn (3 - 22 September 2023). PVC collars with an inner diameter of 245.1 mm, a height of 150 mm, and a wall width of 4.9 mm were inserted into the soil on 29 August 2022. We inserted them as deeply as possible, between 100- 140 mm, to ensure a proper seal between the chamber head space and the atmosphere even during strong wind conditions, and in the palsa where the top peat was dry and highly porous. Between the collar and the chamber, a custom made sealing ring was placed we placed a custom-made sealing ring to avoid ambient air entering the chamber
125 during our measurements (Fig. 2, S2). The sealing ring has an inner and outer diameter 235 and 265 mm, respectively, a height

of 30 mm and is build from a metal ring wrapped in foam material (50 mm on each side). Tests confirmed that it sealed the chamber and the collar even under high wind conditions with up to 18 ms^{-1} wind gusts.

2.2 Chamber and portable gas analyser (PGA) setup and protocol

For our measurements, we used a custom-built static, non-steady state, non-flow-through chamber (Livingston and Hutchinson, 1995) made from acrylic glass (Göli GmbH) with a height of 250 mm and a diameter of 250 mm (Fig. 2, S1). **We placed a** fan (SUNON Maglev, 80 mm x 80 mm x 25 mm, 2000 RPM) **was installed** inside the chamber to ensure well mixed conditions within the chamber during the measurements. Additionally, **we installed** a relative humidity (RH) and temperature probe (EE08, E+E Elektronik, Germany) and a pressure sensor (61402V, RM Young) **were installed** for measuring essential parameters to calculate the fluxes. **The chamber was equipped** **We equipped the chamber** with quick-release connectors on top to connect the inlet and outlet tubing to the portable gas analysers. As complementary variables, we measured soil temperature at 15 cm (PT100 4-wire sensors, JUMO GmbH & Co. KG) at each quadrant outside of the plot, soil moisture at 12 cm and 30 cm (CS655-DS and CS650-DS, Campbell Scientific), and photosynthetically active radiation (PAR) (PQS1, Kipp and Zonen). More detailed information on our chamber setup can be found in the supplementary information.



Figure 2. Chamber setup during measurement period, with soil moisture and soil temperature sensors installed in the soil, and all inlets connected. Photo: Fabio Cian, “Ubiquitous Anomaly”, CC BY-NC-ND 4.0

To measure N_2O concentrations, we used the Aeris MIRA Ultra $\text{N}_2\text{O}/\text{CO}_2$ (from now onward: Aeris- N_2O) analyser (Aeris Technologies; sensitivity: 0.2 ppb/s for CO_2 and N_2O , frequency: 1 Hz). **As most PGAs, the Aeris- N_2O provides dry mole fractions of the target gas.** We performed several laboratory tests to assess the signal stability (*i.e.*, drifts and stabilisation time), uncertainties, noise level, and water interference of the Aeris- N_2O . **The analyser was left to sample ambient air for approximately 15 hrs to evaluate the signal stability (see section 3.1).** Furthermore, we tested the impact of the humidity on the Aeris- N_2O analyser using a portable dew point generator (LI-610, Licor USA). By adjusting the dew point temperature, we examined four different humidity levels: 28, 45, 60, and 83 %. A calibration gas tank with a known N_2O concentration of 333.2 ppb was first connected to the dew

point generator. The humidified gas was then connected to the Aeris-N₂O analyser inlet and each humidity level was sampled for about 20 minutes. Nevertheless, only a 10-minute window was used for further analysis due to relatively long time (about 10 minsmin) required for the humidity levels to stabilise (see Fig. A2).

150 In the field, we attached a custom made external battery box with two LiFePO₄ batteries (LiFePO₄ 12.8V 20Ah, Green Cell) to the Aeris-N₂O, which could be switched whilst the analyser was running. In this study, one LiFePO₄ 12.8V 20Ah battery lasted for the whole day of field measurements (8h - max. 12h). A data logger (CR1000X, Campbell Scientific) was used to log all the sensor data including greenhouse gas concentrations which was placed inside a Pelican-case (Fig. S3 and S4). All GHGs and explanatory variables were logged with a frequency of 1 Hz. With this setup, all necessary information for the analyses was synchronised in a single data file, rather than many individual files from individual sensors and loggers.

155 Before we started a measurement period (*i. e.*, time when chamber is closed), we attached the tubes from the PGA to the chamber, ventilated the chamber for at least one minute, and gently closed it onto the sealing ring. The default chamber closure time for all measurement periods was 10 minutes. For the dark measurements, a custom-made, reflective, light-impermeable tarp, isolating against temperature increases, was placed on top of the chamber. was placed over the chamber to prevent light from entering and minimise temperature fluctuations. We refer to these measurements as 'opaque' for clarity.

160 All data were processed in R (version 4.3.3; R Core Team, 2024) and version controlled in GitLab (the scripts are publicly available from <https://git.bgc-jena.mpg.de/ntriches/data-analysis/-/tags/2024-12-12-triches-amtsubmission-n2oadvances>). A filter script was applied to pre-process and quality-control the raw data (*i.e.*, , and concentrations, chamber pressure, chamber temperature, chamber relative humidity, soil temperature, volumetric water content, and PAR), such as removing data points within a specific time-interval at the start of the data to ensure it met certain quality control standards, including:

- 165
- Removing data from the beginning of each measurement period to account for the time lag of gases moving through the tubes to reach the laser cell, and detecting erroneous data due to instrument failure, seen as flat lines, *i. e.*, periods of exact same concentrations (see SI 1.3). The filter script also included quality control of other parameters by, *e. g.*, removing
 - Removing implausible values (*e. g.*, -9999), replacing of chamber pressure, chamber temperature, chamber relative humidity, soil temperature, volumetric water content, and PAR
 - 170 – Replacing negative PAR values with 0,
 - averaging soil temperature gained from the four sensors, and setting minimum and maximum values for all parameters readings gained from four sensors
 - Detecting and removing flat lines indicating instrument failure (see SI). Furthermore, we used this script to simulate differences between chamber closure times and simulated gas chromatograph (GC) sampling, and the associated sensitivity analysis. 1.3)
 - 175 – Pre-processing data for concentrations of N₂O, CO₂, and H₂O, as well as other relevant parameters.

2.3 Flux calculations

In this study, fluxes were calculated using all data points our study, we calculated N₂O fluxes using all data points from one measurement period. We removed 8 s seconds in the start of the measurement period to account for the time delay until the concentration from the chamber reached the cell of the online laser analysers gas analyser. An extra 7 s were removed for dark opaque measurements, since we needed more time in the field to cover the chamber with the reflective tarp. To calculate the fluxes with both linear (LM) and non-linear (HM) methods in a reproducible way, we used the goFlux R package R package goFlux (v0.2.0, (Rheault et al., 2024)). We selected goFlux for several reasons: (i) it was specifically written to process data gathered with portable analysers PGAs, (ii) it uses measured temperature and pressure inside the chamber for flux calculation, (iii) it corrects for the dissolved gases in the water vapour inside the chamber, and (iv) it calculates fluxes using both LM and HM flux calculation methods. It further allows to compare results gained also enables the comparison of results from LM and HM models through different statistical methods, flags, e. g., using various statistical methods and flags, such as the minimal detectable flux (MDF, Eq. 4), and creates . Additionally, it generates plots for visualisation. For the flux calculation in LM, goFlux applies the commonly used linear equation as follows in Eq. 1:

$$F(t) = \frac{dC(t)}{dt} \frac{V}{A} \quad (1)$$

where $F(t)$ is the gas flux rate at a given location during the chamber closure time (t), $\frac{dC(t)}{dt}$ is the mass concentration change with time, V is the volume of the chamber, and A the area of the soil covered by the collar (Subke et al., 2021). To report our flux rates, we used the atmospheric sign convention, i. e., negative signs for an uptake of N₂O into the soil, and positive signs for emissions.

The HM model approach is based on the Hutchinson and Mosier (1981) approach as given in Eq. 2:

$$C(t) = \varphi + (C_0 - \varphi)e^{-\kappa t} \quad (2)$$

here, φ is the assumed constant gas concentration of the source within the soil (Pedersen et al., 2010), C_0 is the gas concentration in the chamber at the moment of chamber closure, and κ is the model parameter. To limit κ with a maximum threshold κ_{\max} , Eq. 3 was adapted from Hüppi et al. (2018).

$$\kappa_{\max} = \frac{F(t)}{\text{MDF } t} \quad (3)$$

Here, the MDF is used to specify whether the flux estimate was above or below the detection limit which is based on the instrument a theoretical threshold that represents the instrument's detection limit, based on its precision (η) and provided by the manufacturer. However, it does not account for potential errors in the model or chamber artefacts, but reflects the instrument's inherent uncertainty. The MDF can be calculated using Eq. 4.

$$\text{MDF} = \frac{\eta}{t} \theta \quad (4)$$

where, θ is a flux term that corrects for the water vapor vapour inside the chamber and converts the flux unit to $\mu\text{mol m}^{-2} \text{s}^{-1}$
 205 , which and t is the measurement time, i.e., the number of measurement points during the measurement period. This was
 calculated as given in Eq. 5

$$\theta = \frac{(1 - C_{\text{H}_2\text{O}})V P}{A R T} \quad (5)$$

where $C_{\text{H}_2\text{O}}$ is the water vapour concentration in mol mol^{-1} , P is the pressure inside the chamber in kPa, R is the universal
 gas constant in $\text{L kPa K}^{-1} \text{mol}^{-1}$, and T is the air temperature inside the chamber in K.

210 In the goFlux package, the fluxes that are below the detection limit are flagged. Note that owing to this function, all our flux
 estimates have their own MDF value. The package further implements the so called g-factor (g_f) (Hüppi et al., 2018) to restrict
 large curvatures of the non-linear flux models as follows (Eq. 6):

$$g_f = \frac{H M_F}{L M_F} \quad (6)$$

Here, $H M_F$ and $L M_F$ are the flux values that are calculated by HM and LM models, respectively. In this study, we used
 215 a g_f of 4, meaning that the flux calculated by the HM model can be max. 4 times higher than the flux calculated by the LM
 to avoid a large overestimation of fluxes (Eq. 6). We used this factor because it , upon visual assessment, it fit our data best,
 and has been previously used (Leiber-Sauheitl et al., 2014). We did not use the mean absolute error nor the root mean square
 error to define if the HM or LM model performed better, since they were very similar amongst among all measurement periods.
 We did also not use R^2 as a filter criteria since low and non-linear fluxes inherently results in low R^2 values (Kutzbach et al.,
 220 2007).

2.4 Data processing and simulations

We used our openly available script to simulate differences between chamber closure times and gas chromatograph (GC) GC sampling,
 and the associated sensitivity analysis. Firstly, we We first calculated all fluxes with the original using the original 10-minute chamber
 closure time of 10 minutes (prec = 0.2, g.limit = 4). To asses the impact of different chamber closure times on see how different closure times
 225 affect N_2O fluxes, we then removed data points at the end of the original measurements, thus looking at the same measurement periods using the first 3 min, 4 min, 5 min,
 6 min, 7 min, shortened the closure time by 1 minute at a time, starting from 9 minutes, and recalculated the fluxes for each
 new time (e.g., 9 minutes = 540 seconds, 8 min, minutes = 480 seconds, etc.). We compared how chamber closure time
 affects flux rates during transparent and 9 min of the original data. We then explored variations in the flux rates between light (transparent) and dark (opaque)
 measurements as affected by the chamber closure time, and defined opaque measurements, and identified the number of fluxes above the minimal
 230 detectable flux according to minimum detectable flux based on the goFlux output files. While calculating our fluxes, we became aware
 of one chamber base position acting as a hot spot, i. e., showing much higher flux rates than the other chamber base positions.
 Since we wanted to focus our analyses on low fluxes, we removed this hot spot from all analyses.

The simulations of GC measurements are based on drawing discrete sub-samples from the continuous *in situ* time series
 from the PGA, mimicking a sampling scheme where information on the increase of gas concentrations during chamber closure

time is limited to a few snapshots in time. We simulated four scenarios: 3 GC samples (taken at 5 min, 7 min, and 10 min), 4 GC samples (3 min, 5 min, 7 min, and 10 min), 5 GC samples (1 min, 3 min, 5 min, 7 min, and 10 min), and 6 GC samples (1 min, 3 min, 5 min, 7 min, 8 min, and 10 min). For simulating the GC concentration, we picked the time stamp as defined above and took the average of 10 sec of N₂O concentrations measured by the our PGA, *i. e.*, 5 seconds before and after the defined time stamp, as single GC point measurement (Fig. 9). We then calculated the resulting fluxes with goFlux (prec = 1.9, g.limit = 4) using a precision of 1.9 ppb according to sensitivity tests on an instrument at our laboratory (Agilent Technologies, 7890 B GC System, mean N₂O concentration 395.746 ppb with a SD of 1.875 ppb over ten repetitions), before we plotted the simulated versus original flux concentration measurements. To evaluate the performance of each sampling scheme, we compared the slopes, p-values, and R^2 values between the simulations simulated and original data. To get an estimate on the uncertainties associated with this GC simulation, we conducted a sensitivity analysis, where we did 21 simulations with a randomised selection of the 4 min sampling time (4 samples at 3,5,7,9 min), allowing a window of 30 60 sec around each selected GC point.

3 Results and discussion

3.1 Laboratory tests with the Aeris-N₂O

From the 15-hour ambient air sampling in our closed laboratory, we observed that the water vapour mole fraction concentration in the ambient air dropped from approximately 2500 ppm to about 800 ppm within the first 30 min. It continued to decrease progressively throughout the sampling period; however, after 5 hours, the water vapour mole fraction concentration somewhat stabilised, with a mean H₂O concentration of 476.9 ppm with a standard deviation of 18.7 ppm for the rest of the sampling. Note that the these observed changes in water vapour might be partly due to the analysers warming up period. Therefore, we warm-up period. We therefore discarded the initial 5 hours of data and used the remaining data to assess the signal stability and noise characteristics of the Aeris-N₂O. The Aeris-N₂O demonstrated a very stable signal with no apparent drift for about 10 hours of sampling period, having a low standard deviation of 0.324 0.290 ppb. Using Allan deviation plots (Allan, 1987), we evaluated the analyser's noise characteristics and found that the Aeris-N₂O showed low instrument noise, approximately 0.16 0.18 ppb at 2-second averaging (see Fig. 3).

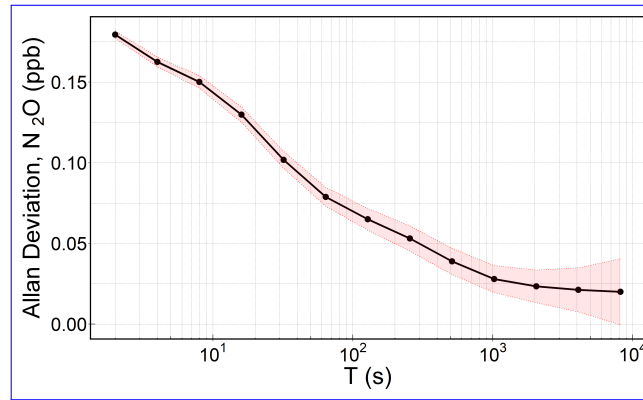


Figure 3. Computed Allan deviation plot based on 10 hours of continuous sampling, following a 5-hr spin up period during which the water vapor vapour mole fraction was not stable. Here, T is the sampling time in log-scale and shaded region represents the 95% confidence interval.

Due to observed relatively high fluctuations under changing water vapor mole fractionBecause PGAs are known to be sensitive to fluctuations in water vapour concentrations, we tested the Aeris-N₂O against different relative humidity (RH) conditions. Our tests with the four RH values (approx. 28%, 45%, 60% and 83%, respectively) showed that the water interference of the Aeris-N₂O was very small; we observed only slight differences were observed in the mean N₂O concentrations for each humidity level (see Fig. 4), with mean N₂O concentrations of 332.7 ppb, 332.6 ppb, 332.7 ppb, and 332.5 ppb for RH values of 28%, 45%, 60%, and 83%, respectively. Furthermore, we observed the same standard deviation of about 0.3 ppb for each humidity level. Overall, the our conducted laboratory tests indicated that the Aeris-N₂O was a suitable instrument for measuring low N₂O fluxes, showing low noise and water interference, along with negligible signal drift after the laser warms up. Nevertheless, the long warm-up period (approximately 5 h) of the analyser needs to be taken into account, as this can be a limiting factor for certain applications. To mitigate this, the Aeris-N₂O remained powered on throughout the whole field campaign.

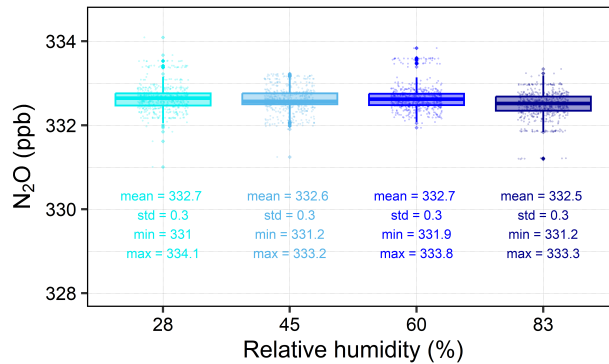


Figure 4. Measured N_2O concentrations for different relative humidity (RH) values, with basic statistics of each RH values summarised under each box plots. Each humidity level was sampled for about approximately 20-mins; however, only a 10-min window was used for further calculations. For our tests, we used a standard gas with a mean of 333.16 ± 0.16 ppb as input. Jittered points are overlaid on the boxplots to visually separate overlapping data points, illustrating the distribution and density of the data.

3.2 Impact of chamber closure time on N_2O fluxes

To report our flux rates, we use negative signs for an uptake of N_2O into the soil, and positive signs for emissions. At our site, we commonly observed net N_2O consumption, suggesting an atmospheric sink, with a mean flux of $-0.469 \pm 1.25 \mu\text{g N}_2\text{O-N m}^{-2} \text{h}^{-1}$ and a 95% confidence interval (CI) of $(-0.60, -0.3)$ during a chamber closure time of 10 min. Separating light and dark measurements, we get Our calculated mean flux during transparent measurements was 0.361 ± 0.797 and $-1.29 \pm 1.07 \mu\text{g N}_2\text{O-N m}^{-2} \text{h}^{-1}$, with a 95% CI of $(0.24, 0.48)$ during a chamber closure time of 10 min, respectively (Table 1). With up to 170 measurement periods for light and dark measurements, i.e., 338 times we closed the chamber to gather a sample, of which nearly 60-90 % of all fluxes were above the minimal detectable flux (Fig. 5), we are confident that the uptake during dark measurements shows an actual biochemical process in the sampled sub-Arctic ecosystem. For opaque measurements, our calculated flux was $-1.29 \mu\text{g N}_2\text{O-N m}^{-2} \text{h}^{-1}$, with a 95% CI of $(-1.45, -1.13)$, indicating that our opaque measurements represent a real biochemical process, rather than an artefact. However, we acknowledge the potential for experimental artefact, in the (sub-) Arctic ecosystem. Nevertheless, the impact of environmental drivers on N_2O fluxes, including the transparent and opaque measurements, is beyond the scope of this study. Overall, we collected 338 samples, with 60-90 % of N_2O fluxes above the detectable limit. We therefore also acknowledge the possibility of unknown chamber artefacts that may remain undiscovered and could affect the interpretation of our data.

Mean flux rates change with chamber closure times because builds up or decreases in the chamber head space. As the closure time increases, the concentration gradient between the soil and the head space decreases, reducing the diffusive flux. Within a closed system, gases can reach a temporary state of equilibrium over time, where the rate of production in the soil balances with the rate of release into the atmosphere. Our results suggest that for light measurements, a chamber closure time of 3 min is too short and may result in significantly different flux rates than longer chamber closure times (ANOVA, $p < 0.05$ for 3 min compared to 8, 9, and 10 min). This discrepancy may be attributed to low microbial activity or the possibility that production is countered by its rapid uptake or dissolution in the water present in the soil matrix, a phenomenon previously observed for (Widén and Lindroth, 2003). From 4 min onward, mean flux rates are not significantly different from one another (data not shown). However, it seems that with a chamber closure time

Table 1. Comparison of chamber closure times for both **light transparent** and **dark opaque** measurements, with SE = Standard Error, **CI** = **confidence interval**, and % = percentage difference between the absolute mean flux of chamber closure time x compared to chamber closure time 10 min. **CI** is the margin of error calculated at 1.96 * SE; the lower CI is calculated as mean flux - CI, the upper CI as mean flux + CI.

heightChamber closure time	Light Transparent / Dark opaque	Mean flux	SD flux	n	SE	CI	lower CI	upper CI	%
height3	light	-0.00	1.54	169	0.12	0.23	-0.24	0.23	98.97
3	dark	-1.49	1.80	170	0.14	0.27	-1.76	-1.22	-15.16
4	light	0.20	1.26	169	0.10	0.19	0.01	0.39	43.58
4	dark	-1.51	1.53	170	0.12	0.23	-1.74	-1.28	-16.92
5	light	0.26	1.06	169	0.08	0.16	0.10	0.42	27.52
5	dark	-1.47	1.39	170	0.11	0.21	-1.68	-1.26	-14.18
6	light	0.30	0.94	169	0.07	0.14	0.16	0.45	16.21
6	dark	-1.43	1.29	170	0.10	0.19	-1.62	-1.24	-10.75
7	light	0.33	0.89	168	0.07	0.14	0.19	0.46	9.41
7	dark	-1.39	1.24	170	0.10	0.19	-1.58	-1.21	-8.05
8	light	0.35	0.83	168	0.06	0.13	0.23	0.48	2.35
8	dark	-1.35	1.21	170	0.09	0.18	-1.54	-1.17	-4.92
9	light	0.36	0.81	168	0.06	0.12	0.24	0.48	1.00
9	dark	-1.34	1.16	170	0.09	0.17	-1.51	-1.17	-3.79
10	light	0.36	0.80	168	0.06	0.12	0.24	0.48	0.00
10	dark	-1.29	1.07	170	0.08	0.16	-1.45	-1.13	0.00

longer than 7 min, the estimated flux is less sensitive to increase during the chamber closure time, with fluxes 10%, 2% and 1% higher between 7 and 10 min compared to 10 min, respectively (Table 1). The proportion of light fluxes exceeding the minimum detectable flux (MDF) increased from 62.7% at a 3-minute closure time to 78.6% at a 10-minute closure time (Fig. 5 a)). This trend suggests that while longer closure times reduce the proportion of fluxes below the MDF and decrease variability, the gain between 4 and 10 min is marginal, with only 5% of fluxes failing to justify significantly prolonged chamber closure duration. It is likely that more observation points and higher concentration change renders the slope of the regression less sensitive to the noise. We thus suggest that for light measurements, depending on chamber size, chamber closure times of more than 4 min lead to reliable flux estimates, with shorter chamber closures having the benefit of disturbing the soil profile for a shorter time.

For dark measurements, we find that the uptake is highest with short chamber closure times, with flux rates around 15% lower at 3 - 5 min than at 10 min, respectively (Table 1). At 6 min, uptake was still 10% higher than at 10 min, decreasing to below 8% between 7 and 9 min. At the same time, the MDF increased from 56.5% to 87.1 between 3 min and 10 min (Fig. 5 b)). Nevertheless, none of the flux rates across different closure times were significantly different from one another (Kruskal-Wallis, p = 0.99). For dark measurements, we thus suggest to keep the chamber closure time between 3-5 min, unless only few data points are available, when aiming for fluxes above the MDF becomes more important.

With the goFlux output, we obtain an individual MDF for each measurement period, allowing us to determine on a case-by-case basis whether a flux is above the MDF. For both light and dark measurements, the MDF in our study was, on average, $0.015 \pm 0.001 \mu\text{mol m}^{-2}\text{h}^{-1}$. This is lower than the reported $0.18 \mu\text{mol m}^{-2}\text{h}^{-1}$ MDF rates in other nutrient-poor ecosystems by Christiansen et al. (2015) (Table 1).

Mean *fluxes* (note: not concentrations) for light and dark measurements, with number of measurement periods above the minimal detectable flux (MDF, %). Note the different y-axes for the upper and lower plots.

While chamber measurements are essential for understanding GHG emissions, they can alter soil-air conditions and introduce observational ~~artifacts~~ **artefacts**. These include potential impacts such as pushing atmospheric air into the soil when closing the chamber, flushing soil gas into the chamber head space, and changing conditions during closure, *e.g.*, ~~increase air~~ **increasing** temperature and humidity **inside the chamber** due to soil and plant evaporation (Subke et al., 2021; Rochette and Eriksen-Hamel, 2008). As a result, the N₂O concentration gradient between the soil and the chamber head space and potentially also the functioning of plants and soil microbes are altered and may cause a bias in the flux estimates (Davidson et al., 2002).

At our site, condensation within the chamber during a measurement period increased drastically with time, especially in the colder months. Although our laboratory tests showed that for the Aeris-N₂O, increased water vapour does not interfere with N₂O concentrations, all laser cells are sensitive to water vapour. Too high water vapour contents can, even with a filter assembly (1 micrometers pore size) within the tube, reach the analyser cell and lead to an abrupt end of a field campaign (Fiedler et al., 2022). ~~Because this is well known, goFlux takes the water vapour changes during a measurement period into account (Rheault et al., 2024). Nevertheless, it is~~ **It is, therefore,** crucial to know how water vapour ~~increase~~ **concentrations vary** over time during chamber closure. At our study site, H₂O concentrations during ~~light~~ **transparent** measurements increased, on average, from below 10000 ppm up to >16000 ppm, depending on the season. When we look at the rate of change over each minute, *i.e.*, 0-1 min, 1-2 min, 2-3 min etc., we can see that this rate of change drastically ~~decreases~~ **decreased** within the first 2 min, and then exponentially ~~decreases~~ **decreased** with increasing chamber closure time (Fig. S5). In other words, H₂O concentrations ~~rise~~ **rose** drastically in the first 2 min (> 1300 ppm; data not shown), after which ~~the level~~ **they levelled** out until around 8 min, before they ~~start~~ **started** increasing again (Fig. S5). For ~~dark~~ **opaque** measurements, the impact ~~follows~~ **followed** the same pattern, but ~~is~~ **was** of much smaller magnitude (approx. 600 ppm rise within the first 2 min; data not shown). ~~However, it is also evident that~~ **Because** the increase of H₂O concentrations ~~does not seem to~~ **did not** directly affect N₂O concentrations in our study (Fig. S5). ~~, and was further considered when calculating the fluxes with goFlux (Rheault et al., 2024), we did not introduce further measures.~~

When ~~transparent chambers are used, there~~ **using transparent chambers, temperature control** is an additional constraint : ~~the temperature within the chamber~~ **(Rochette and Hutchinson, 2015). Ideally, this temperature stays constant during the whole measurement period; however, without any cooling systems attached, this is impossible to achieve** **the chamber temperature remains stable throughout the measurement period. However,** in the field, ~~especially during sunny conditions, this is challenging to achieve without active cooling,~~ **as the chamber** ~~acts like a greenhouse (Fiedler et al., 2022). It is suggested that these temperature increases can lead to an increased microbial activity leading to~~ **'s transparency creates a** **greenhouse effect (Rochette and Hutchinson, 2015). An increase in temperature can enhance microbial activity, leading to either** N₂O production or consumption ~~, resulting in~~ **and potentially causing** biased N₂O concentrations (Rochette and Eriksen-Hamel, 2008; Clough et al., 2020). In our study, ~~we can see a similar pattern for the rate of change of chamber temperatures over time than with the~~ **chamber temperatures during transparent measurements changed similarly to** H₂O concentrations: ~~, with~~ **the strongest decrease happens** **occurring** within the first minutes of the measurement period (Fig. S5 and S6). At our site, temperature increased by around 0.7°C within the first two minutes, which ~~already slows~~ **slowed** down to 0.3°C after 5 min (data not shown). During ~~dark~~ **opaque** measurements, temperature within the chamber ~~even tends to decrease slightly~~ **decreased slightly** by max. 0.2°C in the first

two minutes, and below 0.1°C after three minutes (data not shown). It is likely that during light transparent measurements, the abrupt temperature increase in the first two minutes may impact have impacted N₂O concentrations (Fig. S6); however, cooling systems (Parkin and Venterea, 2010). However, we refrained from using cooling systems such as heat exchangers or ice packs since they also have drawbacks, *e.g.*, causing additional condensation within the chamber (Fiedler et al., 2022)(Clough et al., 2020; Fiedler et al., 2022). As a result, we decided to avoid cooling systems and consider temperature changes cannot exclude potential temperature effects on our N₂O concentrations during our measurement periods. Even though temperature changes are considered in the final flux calculation (Rheault et al., 2024), we argue that temperature changes inside chambers call for shorter closure times.

To minimise disturbances to the soil gas-atmosphere gradient and obtain flux estimates close to pre-deployment levels, several researchers have recommended using short chamber closure times of around 5 minutes (Fiedler et al., 2022; Pavelka et al., 2018; Venterea and Baker, 2008). This is because during chamber closure, mean flux rates vary as N₂O builds up or decreases in the chamber head space (Rochette and Hutchinson, 2015). As closure time increases, the concentration gradient between soil and chamber head space decreases, reducing the diffusive flux. Within a closed system, gases can reach a temporary state of equilibrium over time, where the rate of N₂O production in the soil balances with the rate of N₂O release into the chamber head space(Fiedler et al., 2022). Our results suggest that for transparent measurements, a chamber closure time of 3 min is too short and may result in significantly lower flux rates than longer chamber closure times (ANOVA, $p < 0.05$ for 3 min compared to 8, 9, and 10 min; Fig. 5). This discrepancy may be attributed to low microbial activity, or the possibility that N₂O production is countered by its rapid uptake or dissolution in the water present in the soil matrix, a phenomenon previously observed for CO₂ (Widén and Lindroth, 2003). From 4 min onward, our calculated mean N₂O flux rates are not significantly different from one another (Table 1). The proportion of transparent fluxes above the minimum detectable flux (MDF) increased from 62.7% to 78.6 % as closure time increased from 3 to 10 minutes (Fig. 5 a). While longer closure times reduce uncertainty and the amount of fluxes below the MDF, the gain is small after 4 minutes. We thus recommend chamber closure times of more than 4 minutes for reliable N₂O flux estimates, as this balances the need for accurate transparent measurements while minimising soil disturbance, as well as the impact of increasing temperature on N₂O concentrations within the chamber.

For opaque measurements, we find that our calculated fluxes show higher N₂O uptake from shorter chamber closure times, with flux rates around 15% lower at 3 - 5 min than at 10 min, respectively (Table 1). At 6 min, the differences in our calculated N₂O uptake was still 10% higher than at 10 min, decreasing to below 8% between 7 and 9 min. At the same time, the MDF increased from 56.5% to 87.1% between 3 min and 10 min (Fig. 5 b). Nevertheless, none of the flux rates across different closure times were significantly different from one another (Kruskal-Wallis, $p = 0.99$). Especially for N₂O uptake, it is crucial essential to keep the chamber closure time as short as possible, as the . This is because N₂O availability and its diffusion into the soil are through soil diffusion is often the limiting factor (Liu et al., 2022). This process is driven by the concentration gradient between the atmosphere and the soil: when the for microbial consumption, *i.e.*, atmospheric N₂O consumption by N₂O-reducing microbes (Liu et al., 2022). When the chamber is closed, the N₂O concentration in the chamber head space is decreasing as is taken up head space decreases as it diffuses into the soil, driven by the concentration gradient. As a result, the uptake rate is also decreasing, since

there is less also decreases, since N_2O in the head space reduction may become substrate limited. Consequently, long chamber closure times may underestimate the uptake of atmospheric N_2O molecules. Our analyses . Our analysis of the chamber closure time confirm confirms this: during dark measurements and over all measurement periods opaque measurement, we found that the uptake rate at 3-5 minutes were greatest, and decreased with every minute of added chamber closure time (Fig. 5). In contrast to this, 5). For opaque measurements, we therefore suggest to keep the chamber closure time between 3-5 min, unless very few data points are available, when aiming for fluxes above the MDF becomes more important.

With the goFlux output, we obtain an individual MDF for each measurement period, allowing us to determine on a case-by-case basis if a flux is above the MDF. For both transparent and opaque measurements, the MDF in our study was, on average, $0.03 \mu\text{mol m}^{-2}\text{h}^{-1}$. This is lower than the reported $0.18 \mu\text{mol m}^{-2}\text{h}^{-1}$ MDF rates in other nutrient-poor ecosystems by Christiansen et al. (2015) (Table 1). However, as mentioned above, more than 40% of the fluxes were below the MDF at 3-minute closure time, confirming that these . This confirms that very short closure times may result in can lead to higher uncertainties of flux estimates due to fewer sample points (Christiansen et al., 2015) because the concentration changes are too small to be accurately detected (Fiedler et al., 2022). It is, therefore, crucial essential to consider the precision of the instruments used in the field to identify the best-suited chamber closure time. With the Aeris- N_2O , we recommend chamber closure times between above 4 and 8 min for min for transparent N_2O measurements in low nutrient ecosystems, depending on chamber size and . The optimal closure time depends on factors such as effective chamber height, micro habitat, but also the length and the duration of the field campaign: the shorter the chamber closure time, the more repetitions are possible, resulting in a higher amount of observations . Shorter closure times allow for more repetitions, increasing the number of observation per chamber base position . For dark or adding more replicates, which is essential for the accurate representation of spatial variability (Jungkunst et al., 2018). For opaque measurements, we suggest shorter chamber closure times of 3-5 min. These findings are in line with other studies (Cowan et al., 2014; Kroon et al., 2008; Christiansen et al., 2015) but confirm, for the first time, that these recommendations are applicable to (very) nutrient-poor ecosystems.

3.3 Impact of linear and non-linear flux calculation approaches on N_2O fluxes

To facilitate understanding of how N_2O concentration build-up or reduction in the chamber head space can result in different flux estimates, goFlux automatically produces scatter plots with defined criteria (Fig. 6). These outputs allow for visual control of all measurement periods; additionally, csv outputs with the pre-defined quality checks are automatically produced. Using "best.flux" from Our analysis using the goFlux package . (Rheault et al., 2024) revealed that 59% ($n = 2560$) of all N_2O fluxes during the different chamber closure times were calculated using best described by the HM model, i.e., concentrations showed a indicating non-linear change over time, whilst concentration changes over time. In contrast, 41% ($n = 1728$) were a result of linear (LM) model, i.e., concentrations showed a linear of the fluxes were better explained by the LM model, showing a linear concentration change over time. However, all of the 41% fluxes calculated with the LM model had no HM flux, meaning that the software did not calculate a non-linear flux because the HM model gave the same results as the LM model, and therefore favoured the LM model. In other words, all fluxes were either calculated using the HM model or resulted in the same values as the LM model. This has two possible reasons: the first is that the linearity might be an outcome of short measurement time and low flux, so that the non-

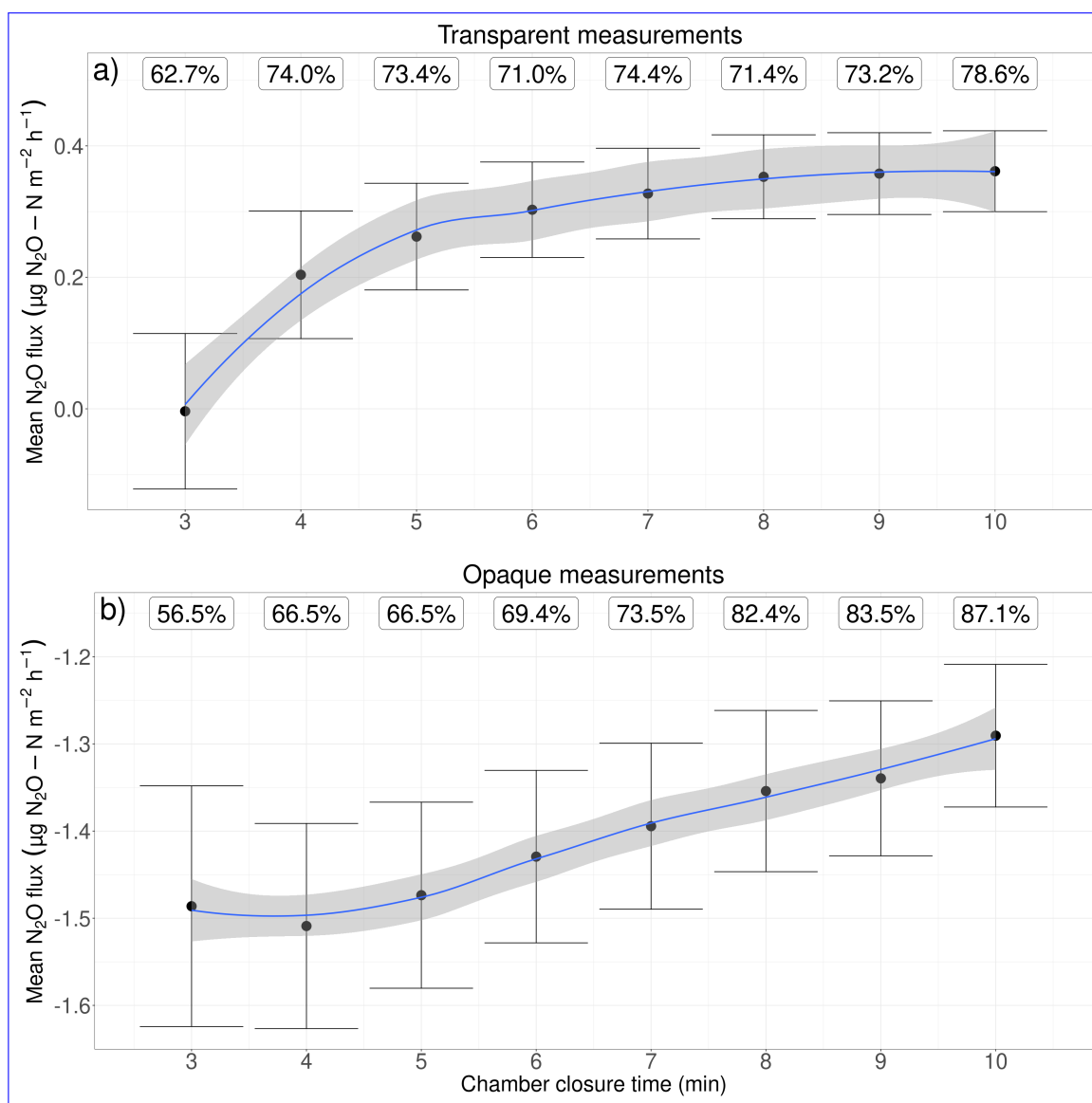


Figure 5. Mean N_2O *fluxes* (note: not concentrations) for transparent and opaque measurements, with number of measurement periods above the minimal detectable flux (MDF, %). Note the different y-axes for the upper and lower plots. The range indicates the upper and lower limit of the 95% confidence interval.

linear model was reduced to a linear model; the second is an overestimation of the flux (Kutzbach et al., 2007). Linear and non-linear fittings to the concentration data, as a function of time during a chamber closure, are often considered to exclude each other. Models for concentration data during chamber closure may typically be seen as alternatives, not complementary approaches. However, the non-linear fitting includes also the linear fitting as a special case. If we use a generic exponential function ae^{-bt} , where a and b to fit data, where a and b are positive constants to be fitted, it is asymptotically reduced to the linear form when b can be approximated to a linear function if the data points are distributed linearly. This is because the exponential function can be expanded as a series, and when the rate constant b is small, the linear function dominates. Namely, the first three terms of the serial expansion are $a(1 - bt + (bt)^2/2)$, and when b is very small, i.e., $b \ll 1$, it is reduced to $a(1 - bt)$, that which is the linear form. The slope of the linear term is readily identified as $-ab$. If we calculate the slope; if we take the time derivative of the original exponential function by taking the time derivative to calculate the slope, it gives $-abe^{-bt}$. Expanding When we expand it as a series and taking only the first order term as $b \ll 1$, we again obtain the simplified $-ab$ as slope. As conclusion, the general (exponential) fitting is automatically reduced to the linear fitting and to its slope if the data points are distributed in a linear manner. Although not novel, this conclusion does not appear to be commonly recognised within the chamber community; with This means that if the data points are linear, the exponential fitting will automatically reduce to a linear fitting with the same slope. With our results, we show that for N_2O fluxes, using a non-linear flux calculation approach yielded better or, for low concentration gradients, indeed, flux estimates were reduced to the linear model and yielded identical results as the linear model. Nevertheless, there is a second reason that linear models are favoured in goFlux: the non-linear model. The second reason for favouring linear models in goFlux is that an unexplained nonlinearity can occur in curvature, i.e., non-exponential curvatures, which can result in an overestimation of the flux estimates (Kutzbach et al., 2007). In goFlux, the curvature of the non-linear model's can be restricted with g_f (see section 2.3). If the curvature was too large, leading to flux estimates over four times higher (with a $g.factor$ $g_f = 4$) than those from the linear model, the linear model was favoured. When we used a lower $g.factor$ g_f of 1.25 for comparison, i.e., allowing HM fluxes to be max. 25% higher than LM, we found that about one-fourth one-quarter of the fluxes estimated by the non-linear model would have been excluded due to significant overestimation.

There is a tendency to favour LM over HM models in literature, primarily due to its their simplicity. It is also generally assumed that concentration changes are linear during short chamber closure times, keeping uncertainties low (Hüppi et al., 2018; Kroon et al., 2008). However, because GHG concentrations naturally follow a non-linear behaviour within a closed system due to diffusion theory (Fick's first law) and leakage (Anthony et al., 1995; Kroon et al., 2008), LM models may introduce a bias, differing from HM model estimates by up to 60% (Hüppi et al., 2018; Kroon et al., 2008), resulting in less accurate flux estimates and GHG budgets. This has been thoroughly investigated for N_2O fluxes by Kroon et al. (2008), who found a large underestimation of N_2O fluxes by the LM model in their study. With our results, including the mathematical explanation stating that LM models are obtained from HM models, we suggest that all future N_2O flux chamber calculations should be done using HM models, which can be filtered for overestimation of fluxes when flux rates are larger. Novel software packages such as goFlux (Rheault et al., 2024) offer the possibility to easily integrate both LM and HM models, and report the flux rates in a reproducible way. We believe that these approaches will be crucial to facilitate the use of both LM and HM models, and, as a consequence, enable the chamber community to standardise their flux calculation methods. We further emphasise the importance of using all available data points for flux estimates, rather than selecting a subset of linear data. This is because our approach, which

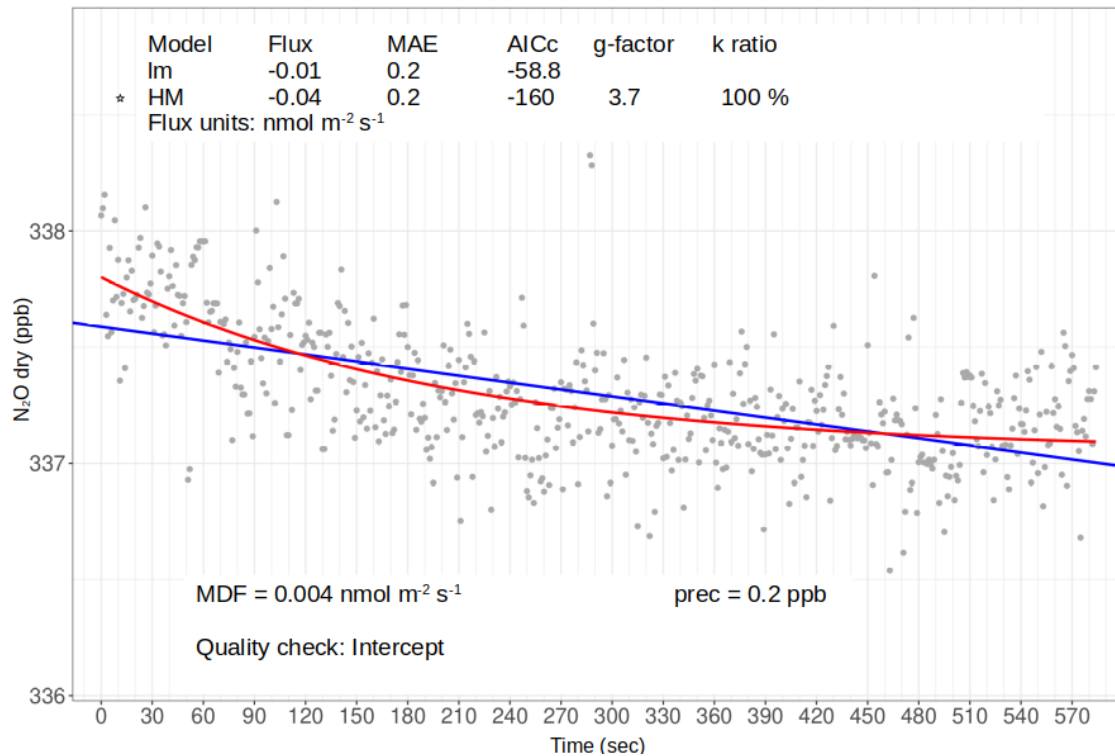


Figure 6. Example of scatterplot output from goFlux, showing N_2O concentrations in ppb from one measurement period, with information on linear (LM, blue line) and non-linear (HM, red line) flux calculations. For every measurement period, the chosen model is marked with a star (here, HM) according to the pre-defined quality check, indicated on the bottom of the graph (here, intercept). Flux values, mean absolute error (MAE), g-factor and k ratio are shown on top of the figure; here, a g-factor of 3.7 indicates that the HM flux value is 3.7 times higher than the one obtained from LM. Source: goFlux package (Rheault et al., 2024), font sizes modified.

involves filtering out unrealistic values and visually verifying measurement periods after flux calculation, enhances the reproducibility and consistency of N_2O flux estimates.

3.4 Simulated differences in N_2O flux rates between GC and PGA

Our results show that for light measurements, indicate that for transparent measurements, the N_2O fluxes obtained with three simulated GC- we
 445 calculated using three simulated GC samples were, on average, 21.7% lower than the PGA fluxes ($0.085 \mu\text{g N}_2\text{O-N m}^{-2}, \text{h}^{-1}$; data not shown) lower than PGA fluxes; especially positive fluxes. Specifically, positive values, i.e., efflux, were generally underestimated ($p < 0.001$, $R_{\text{adj}}^2 = 0.37$, Fig. 7). Using four simulated GC- When we calculated fluxes using four simulated GC samples, negative N_2O fluxes appeared to be nearly identical with the N_2O fluxes gathered by PGA uptake we calculated from the PGA (600 data points); however, positive fluxes were efflux was still underestimated by 3% ($p < 0.001$, $R_{\text{adj}}^2 = 0.65$). Interestingly, by increasing
 450 the sample size to five or six, negative GC-simulated our calculated fluxes seemed to be underestimated, whilst positive ones were underestimate

N₂O uptake, whilst efflux was overestimated ($p < 0.001$, $R^2_{\text{adj}} = 0.85$, Fig. 7). Overall, GC-simulations with the N₂O fluxes we calculated using five samples underestimated N₂O fluxes by 2.2%, while simulations calculations with six samples resulted in an overestimation of around 2.4% (data not shown).

Simulated GC fluxes from light measurements with a) 3, b) 4, c) 5, and d) 6 samples compared to flux measurements taken with a PGA for 10 min ($n = 168$). All fluxes were calculated with the goFlux package; results from "best.Flux" are shown. The blue trend line fits a generalised linear model, with the shaded area representing the 95% confidence interval. The shown equations and R^2_{adj} values follow the $y \sim x$ equation.

For dark For opaque measurements, all N₂O flux estimates gained we calculated from GC simulations were lower than the fluxes measured by estimates we calculated from the PGA, with an underestimation of 6.6%, 2.3%, 7.9%, and 8.1% for three, four, five, and six sample points (data not shown). With three samples, negative fluxes the calculated uptake rates were generally overestimated, while positive fluxes were underestimated. With four sample points, negative fluxes still got efflux was underestimated. When we calculated fluxes using four simulated GC- samples, N₂O uptake was still overestimated, while with five and six sample points, negative fluxes were it was slightly underestimated. However, compared to light transparent measurements, the R^2_{adj} values were low (Fig. 8, $R^2_{\text{adj}} = 0.21, 0.51, 0.69$, and 0.68 , respectively). The underestimation of GC fluxes may occur as a result of a smoothed out curve: when only few data points are available, variations in curves are naturally reduced. Furthermore, the precision of our GC was 1.9 ppb compared to 0.2 ppb of the Aeris-N₂O, resulting in less accurate measurements of the N₂O concentrations. This may lead to a loss of detail in the curve, particularly in the peak values of the N₂O concentrations, which can result in underestimation of the flux.

It is important to note that our comparison was made between our PGA and simulated GC measurements (Figure 9). For the GC simulations, we adjusted the instrument precision during the flux calculation, but no actual air samples were analysed by any GC instrument. Furthermore, our chamber closure time was considerably shorter than for most GC studies because of the condensation and temperature changes within the chamber. During prolonged chamber closure times, significant changes in the concentration gradient and chamber conditions can take place (see above), which are unlikely to be replicated in our GC-simulation. This difference in experimental design may actually be beneficial, as it allows us to isolate and study the effects of shorter closure times on N₂O flux measurements. Furthermore, our sensitivity analysis with 4 simulated GC samples showed that even when we changed the sample times ± 60 sec compared to the original time stamp, flux rates differed less than 10%, with R^2_{adj} values between 92 and 98 (data not shown). We believe that the underestimation of N₂O flux rates we calculated is, therefore, not a result of an inadequate simulation, but needs to be verified by future studies actually measuring N₂O samples from nutrient-poor ecosystems in a GC.

Our results are somewhat similar to previous studies comparing consistent with previous studies that compared N₂O flux rates between GCs and PGAs. These studies found that GCs generally underestimated fluxes compared to fast-responding analysers, but (Fig. 9), which concluded that GCs were still suitable for measuring N₂O fluxes under certain conditions (Christiansen et al., 2015; Brümmer et al., 2017). Christiansen et al. (2015) investigated the differences between a fast-responding analyser (a cavity ring-down spectroscopy analyser (Fleck et al., 2013)) and a high-precision GC in agricultural fields in Vancouver (Canada), with by taking five GC samples at 0, 3, 10, 20, and 30 min chamber closure time. They found that N₂O fluxes were very similar and did not differ significantly, with average N₂O fluxes of $47.6 \pm 8.4 \mu\text{g N}_2\text{O-N m}^{-2} \text{h}^{-1}$ from the the fast-responding analyser and 61.6 ± 11.2

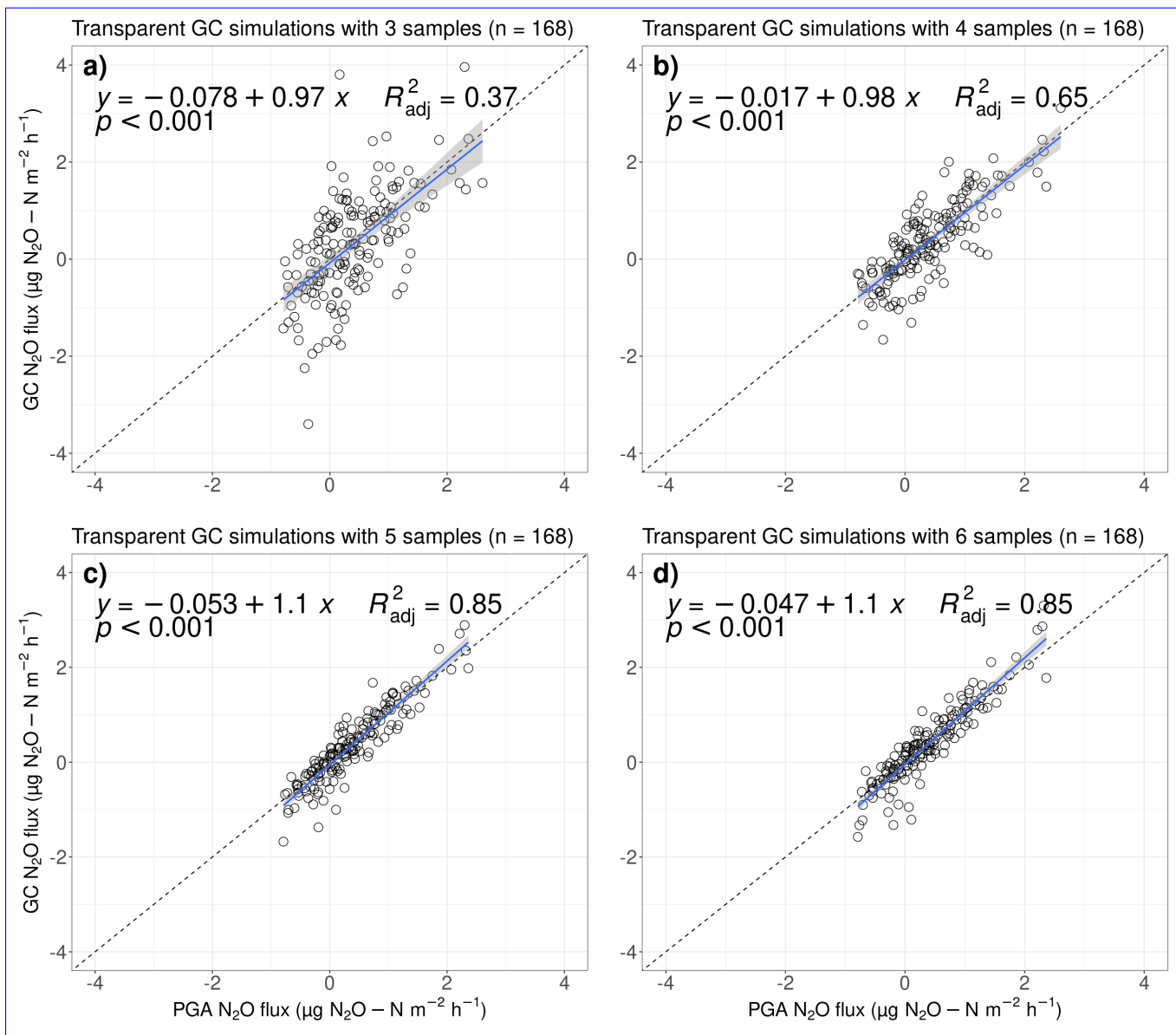


Figure 7. Simulated GC fluxes from **dark light** measurements with a) 3, b) 4, c) 5, and d) 6 samples compared to flux measurements taken with **a blue** PGA for 10 min (n = 338168). All fluxes were calculated with the goFlux package; results from "best.Flux" are shown. The blue trend line fits a generalised linear model, with the shaded area representing the 95% confidence interval. The shown equations and R^2_{adj} values follow the $y \sim x$ equation.

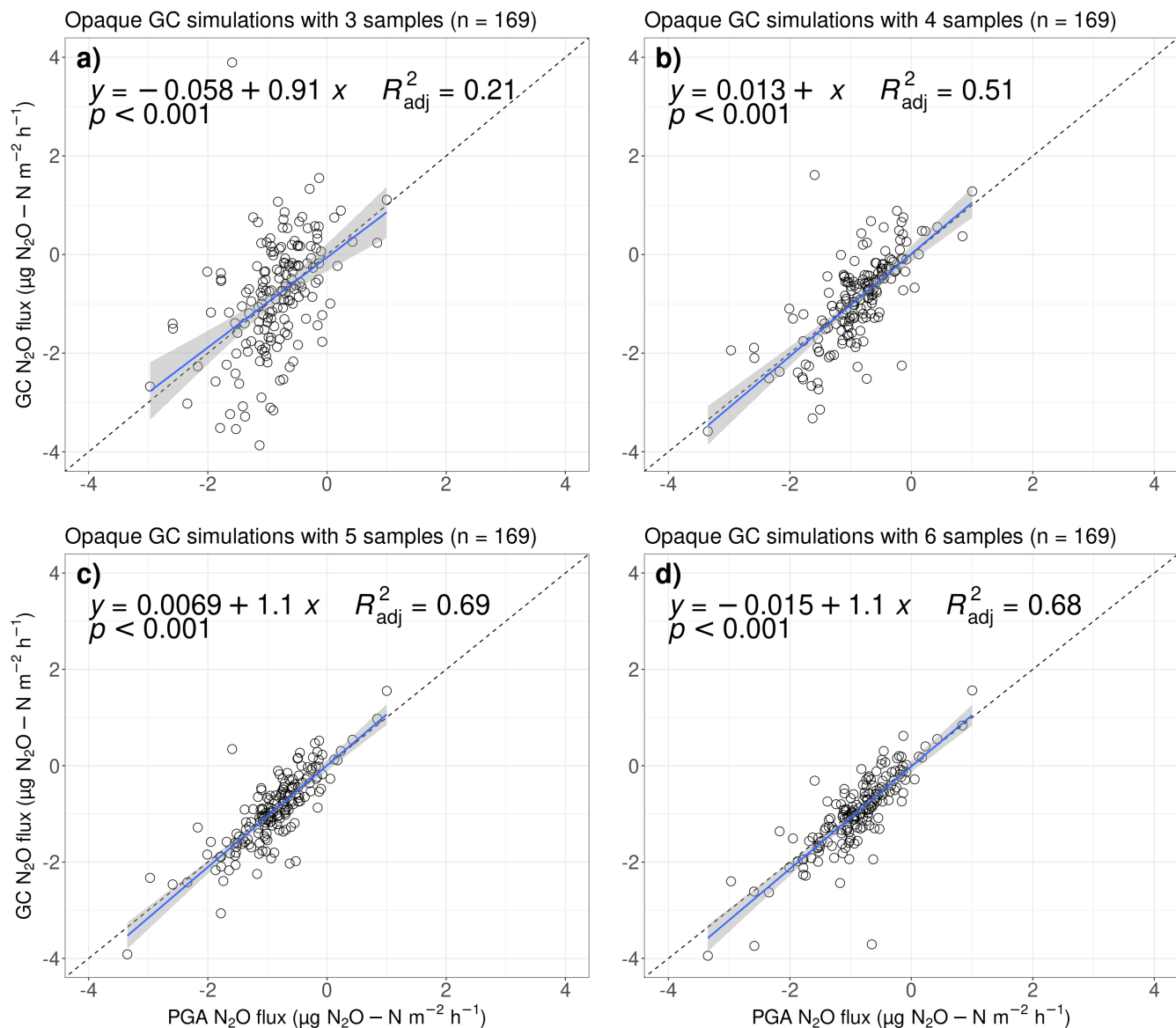


Figure 8. Simulated GC fluxes from opaque measurements with a) 3, b) 4, c) 5, and d) 6 samples compared to flux measurements taken with our PGA for 10 min (n = 338). All fluxes were calculated with the goFlux package; results from "best.Flux" are shown. The blue trend line fits a generalised linear model, with the shaded area representing the 95% confidence interval. The shown equations and R^2_{adj} values follow the $y \sim x$ equation.

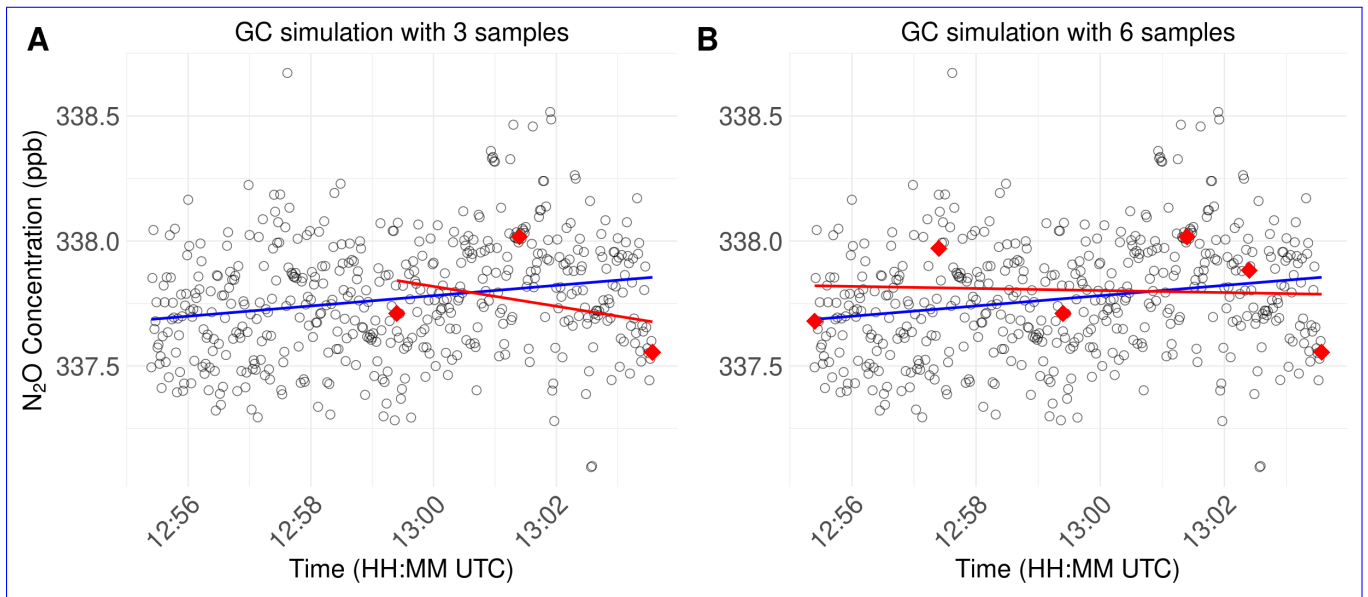


Figure 9. Examples visualising the comparison of regression slopes obtained using 600 data points from the portable gas analyser (blue line) vs 3 (A) or 6 (B) virtual samples mimicking manually defined sample times for subsequent analysis in a gas chromatograph (red line), respectively.

$\mu\text{g N}_2\text{O-N m}^{-2}\text{h}^{-1}$ from GC, respectively. With a similar setup, Brümmer et al. (2017) compared N₂O fluxes measured by a fast-responding analyser similar to the Aeris-N₂O (a quantum cascade laser) and a GC from an low-flux agricultural grassland in Braunschweig (Germany). Their four GC samples taken at 0, 20, 40, and 60 min were highly scattered and rarely showed a distinctive trend, introducing a wide range of N₂O fluxes between -26 to 39 $\mu\text{g N}_2\text{O-N m}^{-2}\text{h}^{-1}$ with a standard error between 1 and 44 $\mu\text{g N}_2\text{O-N m}^{-2}\text{h}^{-1}$. In contrast, the N₂O fluxes measured by the fast-responding analyser only varied between 4 and 32 $\mu\text{g N}_2\text{O-N m}^{-2}\text{h}^{-1}$, with standard errors below 1.2 $\mu\text{g N}_2\text{O-N m}^{-2}\text{h}^{-1}$. It is likely that our results differ because of the short chamber closure time available for our GC simulation, with 10 min compared to 30 min and 60 min in the other studies. During prolonged chamber closure times, substantial changes in the concentration gradient and chamber conditions can take place, which are unlikely to happen in the same extent in our GC-simulation. This highlights three critical aspects: first, despite claiming low-flux environments, flux rates from agricultural fields are much higher than from a sub-Arctic peatland or other nutrient-poor ecosystems (Savage et al., 2014; Cowan et al., 2014), where capturing N₂O fluxes is even more challenging. Second, low N₂O fluxes tend to be very scattered, which with large noise in comparison to the actual trend, *i.e.*, the change in concentration during chamber closure. This makes it very challenging to find trends when calculating fluxes if only few samples are available, let alone showing N₂O uptake without high uncertainties (Cowan et al., 2014). Finally, it is crucial to know and test the precision of the instruments used in the field to get reliable flux estimates and minimal detectable fluxes (Kutzbach et al., 2007; Christiansen et al., 2015).

Our findings suggest that calculating N₂O fluxes from three GC samples is likely to lead to an underestimation of the "real" flux (Kutzbach et al., 2007). We therefore strongly advise against using only three samples, as flux calculations may

have to be discarded if only one sample is erroneous. In contrast, using four to six samples yield very comparable results to those obtained with a PGA, depending on the precision of the GC method. However, the small sample size restricts our ability to confidently identify trends in N_2O fluxes. Undetected errors can bias flux estimates due to the high impact of each data point on the regression slope. To compare previous N_2O flux measurements to novel data sets measured with a PGA, it is crucial to investigate differences between these methods. To achieve this, novel instruments have to be tested on their precision, noise, and accuracy, as well as potential interference with water vapour (Grace et al., 2020; Ahmed et al., 2024).

We suggest that measuring N_2O fluxes with fast-responding analysers in nutrient-poor ecosystems should be considered for all future studies. PGAs, for example, have two main advantages over the GC method: they collect a large amount of sample points, and the quality of these can be checked *in situ* during the measurement period. With more samples, there are more data points, which then results in the option to reduce chamber closure times and further reduce artefacts caused by sealing off a part of a soil profile by a closed chamber (Brümmer et al., 2017). If errors happen in the field, *e.g.*, atmospheric air leaking into the chamber due to not properly closing it, or abrupt pressure changes when closing the chamber to brusquely leakage and pressure change (Rochette and Hutchinson, 2015), they are visible in the online interface of the PGA. This real-time *in situ* control of N_2O concentrations allows for direct optimisation in the field and increases the quality of flux measurements (Fiedler et al., 2022). A practical result of that is that measurement periods can be interrupted and repeated in the field at any time, ensuring high quality of the flux measurements, as well as an optimal use of minimal time in the field, particularly since chamber closure times with PGAs are shorter than with GCs. In addition, most studies using GC have, so far, focussed on soil respiration by only conducting dark measurements; consequently, there is a lack of data on how soil fluxes differ in light and dark conditions, especially in Arctic ecosystems (Stewart et al., 2012), which should be investigated in future studies. However, PGAs have some drawbacks: weighing 10-20 kg (including batteries), they are heavier than GC vials. Additionally, their power consumption requires regular backups, and factors such as heavy vibrations, particles, water, and sudden pressure changes can contaminate the laser cell (Fiedler et al., 2022). With good planning and care, it is, however, easily possible to deal with these disadvantages.

It is important to note that our comparison was made between the PGA and simulated GC measurements. For the GC simulations, we adjusted the instrument precision during the flux calculation, but no actual air samples were analysed by any GC instrument. Furthermore, as mentioned above, our chamber closure time was considerably shorter than for most GC studies because of the condensation and temperature changes within the chamber. Thus, keeping the chamber closure time to max. 10 min proved to be the best solution in our study. Nevertheless, our sensitivity analysis with 4 simulated GC samples showed that even when the sample times changed to ± 30 sec compared to the original time stamp, flux rates differed less than 10%, with R_{adj}^2 values between 92 and 98 (data not shown). We believe that the underestimation of our flux rates is, therefore, not a result of an inadequate simulation, but needs to be verified by future studies actually measuring samples from nutrient-poor ecosystems in a GC. We strongly advise against using only 3 samples, as flux calculations may have to be discarded if only one sample is erroneous. Undetected errors can also bias flux estimates due to the high impact of each data point on the regression slope. To compare previous flux measurements to novel data sets measured with a PGA, it is crucial to investigate differences between these methods. To achieve this, novel instruments have to be tested on their precision, noise, and accuracy, as well as potential interference with water vapour (Grace et al., 2020; Ahmed et al., 2024).

4 Conclusions

The primary aim of this study was to establish a

In our study, we established a manual flux chamber method using a portable gas analyser (PGA) capable of quantifying low N₂O fluxes in nutrient-poor ecosystems . Using a portable analyser (Aeris Technologies; sensitivity: 0.2 ppb/s for and, 1 Hz frequency) and both transparent and dark flux chambers, we generated a first , extensive dataset and, based on our extensive experience with the system, provide detailed practical suggestions on how to collect high-quality measurements in low-flux ecosystems (see SI). To our knowledge, our study represents the first extensive analysis of N₂O fluxes in the (measured with manual flux chambers in a (very) nutrient-poor, (sub-) Arctic ecosystem. Our laboratory tests confirmed the Aeris- that our PGA (Aeris MIRA Ultra N₂O 's suitability / CO₂) is well suited for measuring low N₂O fluxes, with low noise, minimal water interference, and negligible signal drift. Our comparison of chamber closure times (3–10 min) showed that 3 minutes may be insufficient for capturing With our PGA- chamber system, we are able to report very low N₂O fluxes during light measurements, while closure times of 4–10 minutes provide more reliable results, with shorter chamber closures having the benefit of disturbing the soil profile less. For dark measurements, flux values with positive and negative signs, indicating both N₂O uptake was highest with short closure times. We recommend efflux and uptake. Because PGAs allow for near-continuous monitoring of concentration changes with high precision and low detection limits, we recommend, with a chamber height of 25 cm, chamber closure time of 3–5 minutes unless field measurement time data are limited, in which case longer times may help capture fluxes above the MDF. These recommendations should be adjusted based on chamber size, instrument precision, study site, and field campaign duration: shorter closure times allow more repetitions, increasing the number of observations per chamber position. In our study, all fluxes were calculated using the non-linear (HM) model or matched the linear (LM) model when data showed a linear distribution. This occurs because non-linear fitting defaults to linear fitting when concentrations and slopes are low. While not new, this concept is often overlooked in closure times of 3-5 min for opaque and >4 min for transparent measurements to minimise the impacts of the chamber community. Our results demonstrate that the HM model provides the best results or aligns with the LM model for low concentration gradients. We recommend using HM models for future flux calculations , ecosystem due to the measurement setup (e.g., changes in temperature and humidity). To strike a balance between detection sensitivity and measurement efficiency, we suggest using a standard 5-minute closure time for all measurements with smaller chambers, which enables us to detect around 70% of fluxes. This allows for most N₂O fluxes to be detected in this setup; however, the sensitivity depends on the effective chamber height.

We further recommend using non-linear models for N₂O flux calculations (HM; (Hutchinson and Mosier, 1981)), with filters to address overestimation at higher flux rates. Novel software packages such as goFlux (Rheault et al., 2024) simplify the integration of both LM and HM linear and non-linear models, and report flux rates in a reproducible way; such approaches are key to standardising flux calculations across the chamber community. Our simulated comparison between the Aeris- and GC showed that the GC generally underestimated fluxes. Due to the high variability Using non-linear models, as well as standardised and well-documented calculation and quality control, allows to consider the entire time series of measurement periods, and does not require (subjective) expert knowledge to first restrict the datasets to a suitable section, and only afterwards calculate flux estimates. We stress this importance of using all available data points for flux estimates to improve the reproducibility and consistency of N₂O fluxes, we recommend using fast-responding analysers in flux estimates.

We recommend using PGAs in future N₂O studies in nutrient-poor ecosystems . Fast-responding analysers whenever feasible. PGAs collect more data points and allow (typically about 1 sample / second) and allow for real-time *in situ* quality control , enabling optimisation and quality of flux measurements quality control in the field (Fiedler et al., 2022).

570 Our study site, a thawing permafrost peatland in sub-Arctic Sweden, acted as a sink of , with a mean flux of $-0.469 \pm 1.25 \mu\text{g N}_2\text{O-N m}^{-2} \text{h}^{-1}$ during a chamber closure time of 10 min. Light and dark measurements gave 0.361 ± 0.797 and $-1.29 \pm 1.07 \mu\text{g N}_2\text{O-N m}^{-2} \text{h}^{-1}$ during a , while GC measurements may be limited by low flux rates and thus fall below the detection limits or lack clear trends. To get the most out of PGAs, it is essential to determine their precision and use a suitable chamber closure time of 10 min, respectively. With 388 measurement periods for both light and dark measurements, of which up to 90 % of all . In that way, most N_2O fluxes were above the minimal detectable flux, we are confident that this uptake reflects a real biochemical process rather than an artefact. can be detected, which is especially important in nutrient-poor ecosystems, where N_2O fluxes are often very low. Future studies using other chamber designs may benefit from re-evaluating chamber closure times and flux calculation methods to find optimum customised setups.

575 While this study concentrates on the methodological aspects of quantifying N_2O fluxes in a nutrient-poor ecosystem, a follow-up study will investigate the environmental drivers of N_2O fluxes. Our results demonstrate that low Because most studies in the (sub-) Arctic have reported N_2O fluxes can be measured in the Arctic, with from opaque measurements only, there is a lack of data on how soil N_2O fluxes differ in various light conditions, especially in Arctic ecosystems (Stewart et al., 2012). Our results demonstrate notable differences between light and dark transparent and opaque conditions that require further investigation. This fills an important gap in N_2O studies from the Arctic, where negative fluxes have been observed, but could not be investigated due to measurement accuracy not being high enough (Voigt et al., 2020). It also Further, this novel finding highlights the need for future research on N_2O fluxes in sub-Arctic ecosystems and other nutrient-poor ecosystems, and their potential response to global warming.

Code availability. The scripts for processing and analysing the data are publicly available at <https://git.bgc-jena.mpg.de/ntriches/data-analysis/-/tags/2024-12-12-triches-amtsubmission-n2oadvances> under the terms of the GNU General Public License version 3.

Appendix A

590 Sampling ambient air using Aeris- N_2O analyser, Fig. A1 shows the entire 15 hours long run without removing the first 5 hours (1 Hz), where the water vapour mole fractions were not stable.

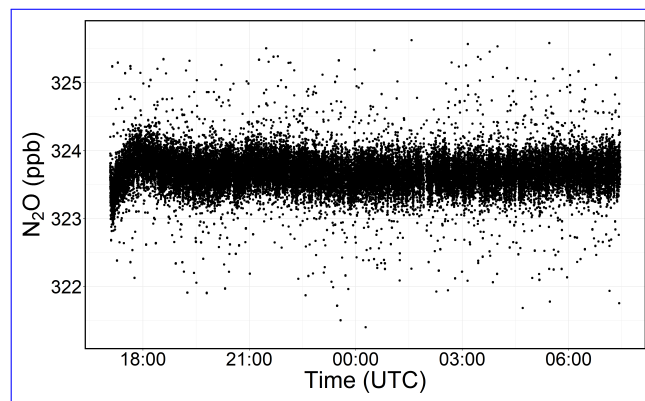


Figure A1. Time series of the N₂O-Analyser of 15 hrs long run.

Changes of H₂O mole fractions during the water interference test (see Fig. A2). Corresponding relative humidity values were noted and the data used for the comparison were designated with red vertical lines.

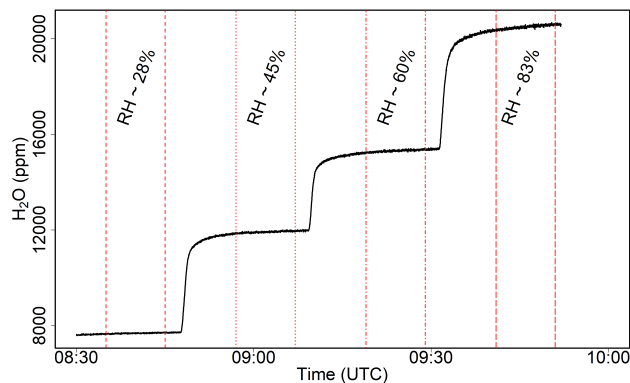


Figure A2. H₂O mole fractions measured by Aeris-N₂O analyser during the water interference test. The corresponding relative humidity (RH) values were given for each step. Red lines demonstrate the data used to assess the water interference at each RH steps.

595 Examples visualising the comparison of regression slopes obtained using 600 data points from the portable gas analyser (blue line) vs 3 (A) or 6 (B) virtual samples mimicking manually defined sample times for subsequent analysis in a gas chromatograph (red line), respectively.

Author contributions. NYT designed the experiment, collected, and processed the data, and did the laboratory test together with AB. AB further analysed and reported the laboratory data, and created the QGIS figures. NYT and JE developed and implemented the scripts used for data processing, quality checks, analysis, and GC simulations. TV wrote the mathematical explanation of non-linear and linear models. NYT wrote the first draft of the manuscript, and AB, AMV, MEM, MG, MH and TV provided valuable comments that helped improving it. NYT was supervised by MG, MH, TV, AMV, and MEM. MH and MG were responsible for funding acquisition.

Competing interests. The authors declare that they have no conflict of interest.

Acknowledgements. The presented research was supported by the European Research Council (ERC) under the European Union's Horizon 2020 research and innovation programme (grant agreement No 951288, Q-Arctic) and by ICOS-Finland (University of Helsinki). The work of MEM was financed by Research Council of Finland-funded projects Thaw-N (no. 353858) and N-Perm (no. 341348). AMV acknowledges
605 funding catalyzed by the TED Audacious Project (Permafrost Pathways).

The authors thank the 'Field experiments & instrumentation' and ', 'Mechanical and electronics workshops' and 'GasLab' service groups at the Max Planck Institute for Biogeochemistry for their help in designing the chamber system and testing the Aeris-N₂O. We also thank Christina Biasi and Richard Lamprecht who helped with the experiment design and setup. Further thanks to the field assistants Alena Markelova, Antonin Affolder, Mark Schlutow, Mirkka Rovamo, Valentin Kriegel and Wasi Hashmi, as well as the staff from the Abisko
610 Scientific Research Station and Mattias Dalkvist. Many thanks to Karelle Rheault for her continuous help with the goFlux package, and Jesper Christiansen for support in the interpretation of non-linear and linear flux rates. Authors also thank Danilo Custódio and Nicholas J. Eves at MPI-BGC/BSI for his their valuable comments and suggestions which helped us to improve this manuscript.

References

- Ahmed, W., Osborne, E. L., Veluthandath, A. V., and Senthil Murugan, G.: A Rapid and Simplified Approach to Correct Atmospheric
615 Absorptions in Infrared Spectra, *Analytical Chemistry*, p. acs.analchem.4c03594, <https://doi.org/10.1021/acs.analchem.4c03594>, 2024.
- Allan, D. W.: Should the Classical Variance Be Used As a Basic Measure in Standards Metrology?, *IEEE TRANSACTIONS ON INSTRUMENTATION AND MEASUREMENT*, 36, 1987.
- Anthony, W. H., Hutchinson, G. L., and Livingston, G. P.: Chamber Measurement of Soil-Atmosphere Gas Exchange: Linear vs. Diffusion-Based Flux Models, *Soil Science Society of America Journal*, 59, 1308–1310,
620 <https://doi.org/10.2136/sssaj1995.03615995005900050015x>, 1995.
- Brümmer, C., Lyshede, B., Lempio, D., Delorme, J.-P., Rüffer, J. J., Fuß, R., Moffat, A. M., Hurkuck, M., Ibrom, A., Ambus, P., Flessa, H., and Kutsch, W. L.: Gas chromatography vs. quantum cascade laser-based N₂ and O₂ flux measurements using a novel chamber design, *Biogeosciences*, 14, 1365–1381, <https://doi.org/10.5194/bg-14-1365-2017>, 2017.
- Buchen, C., Roobroeck, D., Augustin, J., Behrendt, U., Boeckx, P., and Ulrich, A.: High N₂O Consumption Potential of
625 Weakly Disturbed Fen Mires with Dissimilar Denitrifier Community Structure, *Soil Biology and Biochemistry*, 130, 63–72, <https://doi.org/10.1016/j.soilbio.2018.12.001>, 2019.
- Callaghan, T. V., Jonasson, C., Thierfelder, T., Yang, Z., Hedenås, H., Johansson, M., Molau, U., Van Bogaert, R., Michelsen, A., Olofsson, J., Gwynn-Jones, D., Bokhorst, S., Phoenix, G., Bjerke, J. W., Tømmervik, H., Christensen, T. R., Hanna, E., Koller, E. K., and Sloan, V. L.: Ecosystem change and stability over multiple decades in the Swedish subarctic: complex processes and multiple drivers, *Philosophical
630 Transactions of the Royal Society B: Biological Sciences*, 368, 20120488, <https://doi.org/10.1098/rstb.2012.0488>, 2013.
- Christensen, T. R., Michelsen, A., and Jonasson, S.: Exchange of CH₄ and N₂O in a subarctic heath soil: effects of inorganic N and P and amino acid addition, *Soil Biology and Biochemistry*, 31, 637–641, 1999.
- Christiansen, J. R., Outhwaite, J., and Smukler, S. M.: Comparison of CO₂, CH₄ and N₂O soil-atmosphere exchange measured in static chambers with cavity ring-down spectroscopy and gas chromatography, *Agricultural and Forest Meteorology*, 211–212, 48–57,
635 <https://doi.org/10.1016/j.agrformet.2015.06.004>, 2015.
- Clough, T. J., Rochette, P., Thomas, S. M., Pihlatie, M., Christiansen, J. R., and Thorman, R. E.: Global Research Alliance N₂ O chamber methodology guidelines: Design considerations, *Journal of Environmental Quality*, 49, 1081–1091, <https://doi.org/10.1002/jeq2.20117>, 2020.
- Cowan, N. J., Famulari, D., Levy, P. E., Anderson, M., Bell, M. J., Rees, R. M., Reay, D. S., and Skiba, U. M.: An improved method for
640 measuring soil N_2O fluxes using a quantum cascade laser with a dynamic chamber, *European Journal of Soil Science*, 65, 643–652, <https://doi.org/10.1111/ejss.12168>, 2014.
- Davidson, E. A., Savage, K., Verchot, L. V., and Navarro, R.: Minimizing artifacts and biases in chamber-based measurements of soil respiration, *Agricultural and Forest Meteorology*, 113, 21–37, [https://doi.org/10.1016/S0168-1923\(02\)00100-4](https://doi.org/10.1016/S0168-1923(02)00100-4), number: 1, 2002.
- De Klein, C. A. M., Harvey, M. J., Clough, T. J., Petersen, S. O., Chadwick, D. R., and Venterea, R. T.: Global Research Alliance N₂ O
645 chamber methodology guidelines: Introduction, with health and safety considerations, *Journal of Environmental Quality*, 49, 1073–1080, <https://doi.org/10.1002/jeq2.20131>, 2020.
- Denmead, O. T.: Approaches to measuring fluxes of methane and nitrous oxide between landscapes and the atmosphere, *Plant and Soil*, 309, 5–24, <https://doi.org/10.1007/s11104-008-9599-z>, number: 1-2, 2008.

- Elberling, B., Christiansen, H. H., and Hansen, B. U.: High nitrous oxide production from thawing permafrost, *Nature Geoscience*, 3, 332–335, <https://doi.org/10.1038/ngeo803>, 2010.
- Fiedler, J., Fuß, R., Glatzel, S., Hagemann, U., Huth, V., Jordan, S., Jurasinski, G., Kutzbach, L., Maier, M., Schäfer, K., Weber, T., and Weymann, D.: BEST PRACTICE GUIDELINE: Measurement of carbon dioxide, methane and nitrous oxide fluxes between soil-vegetation-systems and the atmosphere using non-steady state chambers, 2022.
- Fleck, D., He, Y., Herman, D., Moseman-valtierra, S., and Jacobson, G. A.: Comparison of a Gas Chromatograph and a Cavity Ringdown Spectrometer for Flux Quantification of Nitrous Oxide, Carbon Dioxide and Methane in Closed Soil Chambers Derek Fleck¹, Yonggang He¹, Donald Herman², Serena Moseman-Valtierra³, Gloria Jacobson¹ ¹ Picarro Inc, 3105 Patrick Henry Drive, Santa Clara, CA 95054 ² College of Natural Resource, UC Berkeley, 130 Mulford Hall, University of California, Berkeley, CA, 94720-3114 ³ University of Rhode Island, CBLS 489, Kingston, RI 02881, 2013, B11F-0428, <https://ui.adsabs.harvard.edu/abs/2013AGUFM.B11F0428F>, conference Name: AGU Fall Meeting Abstracts ADS Bibcode: 2013AGUFM.B11F0428F, 2013.
- Grace, P. R., Weerden, T. J., Rowlings, D. W., Scheer, C., Brunk, C., Kiese, R., Butterbach-Bahl, K., Rees, R. M., Robertson, G. P., and Skiba, U. M.: Global Research Alliance N₂O chamber methodology guidelines: Considerations for automated flux measurement, *Journal of Environmental Quality*, 49, 1126–1140, <https://doi.org/10.1002/jeq2.20124>, number: 5, 2020.
- Grogan, P., Michelsen, A., Ambus, P., and Jonasson, S.: Freeze–thaw regime effects on carbon and nitrogen dynamics in sub-arctic heath tundra mesocosms, *Soil Biology and Biochemistry*, 36, 641–654, <https://doi.org/10.1016/j.soilbio.2003.12.007>, 2004.
- Hensen, A., Skiba, U., and Famulari, D.: Low cost and state of the art methods to measure nitrous oxide emissions, *Environmental Research Letters*, 8, 025 022, <https://doi.org/10.1088/1748-9326/8/2/025022>, 2013.
- Hutchinson, G. L. and Mosier, A. R.: Improved Soil Cover Method for Field Measurement of Nitrous Oxide Fluxes, *SOIL SCI. SOC. AM. J.*, 45, 6, 1981.
- Hübschmann, H.: Handbook of GC-MS: Fundamentals and Applications, Wiley, 1 edn., ISBN 978-3-527-33474-2 978-3-527-67430-5, <https://doi.org/10.1002/9783527674305>, 2015.
- Hüppi, R., Felber, R., Krauss, M., Six, J., Leifeld, J., and Fuß, R.: Restricting the nonlinearity parameter in soil greenhouse gas flux calculation for more reliable flux estimates, *PLOS ONE*, 13, e0200876, <https://doi.org/10.1371/journal.pone.0200876>, publisher: Public Library of Science (PLoS), 2018.
- IPCC: Climate Change 2021 – The Physical Science Basis: Working Group I Contribution to the Sixth Assessment Report of the Intergovernmental Panel on Climate Change, Cambridge University Press, 1 edn., ISBN 978-1-009-15789-6, <https://doi.org/10.1017/9781009157896>, 2023.
- Jonasson, C., Sonesson, M., Christensen, T. R., and Callaghan, T. V.: Environmental Monitoring and Research in the Abisko Area—An Overview, *AMBIO*, 41, 178–186, <https://doi.org/10.1007/s13280-012-0301-6>, 2012.
- Jungkunst, H. F., Meurer, K. H. E., Jurasinski, G., Niehaus, E., and Günther, A.: How to Best Address Spatial and Temporal Variability of Soil-derived Nitrous Oxide and Methane Emissions, *Journal of Plant Nutrition and Soil Science*, 181, 7–11, <https://doi.org/10.1002/jpln.201700607>, 2018.
- Kroon, P. S., Hensen, A., Van Den Bulk, W. C. M., Jongejan, P. A. C., and Vermeulen, A. T.: The importance of reducing the systematic error due to non-linearity in N₂O flux measurements by static chambers, *Nutrient Cycling in Agroecosystems*, 82, 175–186, <https://doi.org/10.1007/s10705-008-9179-x>, 2008.

- 685 Kutzbach, L., Schneider, J., Sachs, T., Giebels, M., Nykänen, H., Shurpali, N. J., Martikainen, P. J., Alm, J., and Wilmking, M.: CO₂ flux determination by closed-chamber methods can be seriously biased by inappropriate application of linear regression, *Biogeosciences*, 4, 1005–1025, <https://doi.org/10.5194/bg-4-1005-2007>, 2007.
- Leiber-Sauheitl, K., Fuß, R., Voigt, C., and Freibauer, A.: High CO₂ fluxes from grassland on histic Gleysol along soil carbon and drainage gradients, *Biogeosciences*, 11, 749–761, <https://doi.org/10.5194/bg-11-749-2014>, 2014.
- 690 Liu, H., Li, Y., Pan, B., Zheng, X., Yu, J., Ding, H., and Zhang, Y.: Pathways of soil N₂O uptake, consumption, and its driving factors: a review, *Environmental Science and Pollution Research*, 29, 30 850–30 864, <https://doi.org/10.1007/s11356-022-18619-y>, 2022.
- Livingston, G. P. and Hutchinson, G. L.: Enclosure-based measurement of trace gas exchange: applications and sources of error, in: *Biogenic Trace Gases: Measuring Emissions from Soil and Water* (P.A. Matson and R.C. Harriss (eds.)), pp. 14–51, John Wiley & Sons, ISBN 978-1-4443-1381-9, google-Books-ID: WDjpgK7IQAgC, 1995.
- 695 Lundin, E., Crill, P., Grudd, H., Holst, J., Kristoffersson, A., Meire, A., Mölder, M., and Rakos, N.: ETC L2 ARCHIVE, Abisko-Stordalen Palsa Bog, 2022-01-01–2024-09-01, <https://hdl.handle.net/11676/e22P1IhSEko3C-2eEIZrVMf6>, 2024.
- Malmer, N., Johansson, T., Olsrud, M., and Christensen, T. R.: Vegetation, climatic changes and net carbon sequestration in a North-Scandinavian subarctic mire over 30 years, *Global Change Biology*, 11, 1895–1909, <https://doi.org/10.1111/j.1365-2486.2005.01042.x>, 2005.
- 700 Martikainen, P. J., Nykänen, H., Crill, P., and Silvola, J.: Effect of a Lowered Water Table on Nitrous Oxide Fluxes from Northern Peatlands, *Nature*, 366, 51–53, <https://doi.org/10.1038/366051a0>, 1993.
- Marushchak, M. E., Pitkämäki, A., Koponen, H., Biasi, C., Seppälä, M., and Martikainen, P. J.: Hot spots for nitrous oxide emissions found in different types of permafrost peatlands: NITROUS OXIDE FLUXES FROM PERMAFROST PEATLANDS, *Global Change Biology*, 17, 2601–2614, <https://doi.org/10.1111/j.1365-2486.2011.02442.x>, 2011.
- 705 Myhre, G., Shindell, D., Bréon, F.-M., Collins, W., Fuglestedt, J., Huang, J., Koch, D., Lamarque, J.-F., Lee, D., Mendoza, B., Nakajima, T., Robock, A., Stephens, G., Zhang, H., Aamaas, B., Boucher, O., Dalsøren, S. B., Daniel, J. S., Forster, P., Granier, C., Haigh, J., Hodnebrog, , Kaplan, J. O., Marston, G., Nielsen, C. J., O'Neill, B. C., Peters, G. P., Pongratz, J., Ramaswamy, V., Roth, R., Rotstayn, L., Smith, S. J., Stevenson, D., Vernier, J.-P., Wild, O., Young, P., Jacob, D., Ravishankara, A. R., and Shine, K.: Anthropogenic and Natural Radiative Forcing, in: *Climate Change 2013: The Physical Science Basis. Contribution of Working Group I to the Fifth Assessment Report of the Intergovernmental Panel on Climate Change* [Stocker, T.F., D. Qin, G.-K. Plattner, M. Tignor, S.K. Allen, J. Boschung, A. Nauels, Y. Xia, V. Bex and P.M. Midgley (eds.)], p. 82, Cambridge University Press, Cambridge, United Kingdom and New York, USA, https://www.ipcc.ch/site/assets/uploads/2018/02/WG1AR5_Chapter08_FINAL.pdf, 2013.
- 710 Parkin, T. B. and Venterea, R. T.: USDA-ARS GRACEnet project protocols, chapter 3. Chamber-based trace gas flux measurements, Sampling protocols. Beltsville, MD p. pp. 1–39, 2010.
- 715 Pavelka, M., Acosta, M., Kiese, R., Altimir, N., Brümmer, C., Crill, P., Darenova, E., Fuß, R., Gielen, B., Graf, A., Klemetsson, L., Lohila, A., Longdoz, B., Lindroth, A., Nilsson, M., Jiménez, S. M., Merbold, L., Montagnani, L., Peichl, M., Pihlatie, M., Pumpanen, J., Ortiz, P. S., Silvennoinen, H., Skiba, U., Vestin, P., Weslien, P., Janous, D., and Kutsch, W.: Standardisation of chamber technique for CO₂, N₂O and CH₄ fluxes measurements from terrestrial ecosystems, *International Agrophysics*, 32, 569–587, <https://doi.org/10.1515/intag-2017-0045>, number: 4, 2018.
- 720 Pedersen, A. R., Petersen, S. O., and Schelde, K.: A comprehensive approach to soil-atmosphere trace-gas flux estimation with static chambers, *European Journal of Soil Science*, 61, 888–902, <https://doi.org/10.1111/j.1365-2389.2010.01291.x>, 2010.

- Pumpanen, J., Kolari, P., Ilvesniemi, H., Minkkinen, K., Vesala, T., Niinistö, S., Lohila, A., Larmola, T., Morero, M., Pihlatie, M., Janssens, I., Yuste, J. C., Grünzweig, J. M., Reth, S., Subke, J.-A., Savage, K., Kutsch, W., Østreng, G., Ziegler, W., Anthoni, P., Lindroth, A., and Hari, P.: Comparison of Different Chamber Techniques for Measuring Soil CO₂ Efflux, *Agricultural and Forest Meteorology*, 123, 159–176, <https://doi.org/10.1016/j.agrformet.2003.12.001>, 2004.
- Repo, M. E., Susiluoto, S., Lind, S. E., Jokinen, S., Elsakov, V., Biasi, C., Virtanen, T., and Martikainen, P. J.: Large N₂O emissions from cryoturbated peat soil in tundra, *Nature Geoscience*, 2, 189–192, <https://doi.org/10.1038/ngeo434>, 2009.
- Rheault, K., Christiansen, J. R., and Larsen, K. S.: goFlux: A user-friendly way to calculate GHG fluxes yourself, regardless of user experience, *Journal of Open Source Software*, 9, 6393, <https://doi.org/10.21105/joss.06393>, 2024.
- Rochette, P. and Eriksen-Hamel, N. S.: Chamber Measurements of Soil Nitrous Oxide Flux: Are Absolute Values Reliable?, *Soil Science Society of America Journal*, 72, 331–342, <https://doi.org/10.2136/sssaj2007.0215>, 2008.
- Rochette, P. and Hutchinson, G. L.: Measurement of Soil Respiration in Situ: Chamber Techniques, in: *Agronomy Monographs*, edited by Hatfield, J. and Baker, J., pp. 247–286, American Society of Agronomy, Crop Science Society of America, and Soil Science Society of America, Madison, WI, USA, ISBN 978-0-89118-268-9 978-0-89118-158-3, <https://doi.org/10.2134/agronmonogr47.c12>, 2015.
- Savage, K., Phillips, R., and Davidson, E.: High temporal frequency measurements of greenhouse gas emissions from soils, *Biogeosciences*, 11, 2709–2720, <https://doi.org/10.5194/bg-11-2709-2014>, number: 10, 2014.
- Schlesinger, W. H.: An Estimate of the Global Sink for Nitrous Oxide in Soils, *Global Change Biology*, 19, 2929–2931, <https://doi.org/10.1111/gcb.12239>, 2013.
- Siewert, M. B.: High-resolution digital mapping of soil organic carbon in permafrost terrain using machine learning: a case study in a sub-Arctic peatland environment, *Biogeosciences*, 15, 1663–1682, <https://doi.org/10.5194/bg-15-1663-2018>, 2018.
- Sjögersten, S., Ledger, M., Siewert, M., De La Barreda-Bautista, B., Sowter, A., Gee, D., Foody, G., and Boyd, D. S.: Optical and radar Earth observation data for upscaling methane emissions linked to permafrost degradation in sub-Arctic peatlands in northern Sweden, *Biogeosciences*, 20, 4221–4239, <https://doi.org/10.5194/bg-20-4221-2023>, 2023.
- Stewart, K. J., Brummell, M. E., Farrell, R. E., and Siciliano, S. D.: N₂O flux from plant-soil systems in polar deserts switch between sources and sinks under different light conditions, *Soil Biology and Biochemistry*, 48, 69–77, <https://doi.org/10.1016/j.soilbio.2012.01.016>, 2012.
- Subke, J.-A., Kutzbach, L., and Risk, D.: Soil Chamber Measurements, in: *Springer Handbook of Atmospheric Measurements*, edited by Foken, T., pp. 1603–1624, Springer International Publishing, Cham, ISBN 978-3-030-52170-7 978-3-030-52171-4, https://doi.org/10.1007/978-3-030-52171-4_60, series Title: Springer Handbooks, 2021.
- Thoning, K., Dlugokencky, E., Lan, X., and NOAA Global Monitoring Laboratory: Trends in globally-averaged CH₄, N₂O, and SF₆, <https://doi.org/10.15138/P8XG-AA10>, 2022.
- Varner, R. K., Crill, P. M., Frolking, S., McCalley, C. K., Burke, S. A., Chanton, J. P., Holmes, M. E., Isogenie Project Coordinators, Saleska, S., and Palace, M. W.: Permafrost thaw driven changes in hydrology and vegetation cover increase trace gas emissions and climate forcing in Stordalen Mire from 1970 to 2014, *Philosophical Transactions of the Royal Society A: Mathematical, Physical and Engineering Sciences*, 380, 20210022, <https://doi.org/10.1098/rsta.2021.0022>, 2022.
- Venterea, R. T. and Baker, J. M.: Effects of Soil Physical Nonuniformity on Chamber-Based Gas Flux Estimates, *Soil Science Society of America Journal*, 72, 1410–1417, <https://doi.org/10.2136/sssaj2008.0019>, 2008.
- Virkkala, A.-M., Niittynen, P., Kempainen, J., Marushchak, M. E., Voigt, C., Hensgens, G., Kerttula, J., Happonen, K., Tyystjärvi, V., Biasi, C., Hultman, J., Rinne, J., and Luoto, M.: High-resolution spatial patterns and drivers of terrestrial ecosystem carbon dioxide, methane, and nitrous oxide fluxes in the tundra, *Biogeosciences*, 21, 335–355, <https://doi.org/10.5194/bg-21-335-2024>, 2024.

- 760 Voigt, C., Marushchak, M. E., Abbott, B. W., Biasi, C., Elberling, B., Siciliano, S. D., Sonnentag, O., Stewart, K. J., Yang, Y., and Martikainen, P. J.: Nitrous oxide emissions from permafrost-affected soils, *Nature Reviews Earth & Environment*, 1, 420–434, <https://doi.org/10.1038/s43017-020-0063-9>, 2020.
- Widén, B. and Lindroth, A.: A Calibration System for Soil Carbon Dioxide-Efflux Measurement Chambers: Description and Application, *Soil Science Society of America Journal*, 67, 327–334, <https://doi.org/10.2136/sssaj2003.3270>, 2003.
- 765 Łakomiec, P., Holst, J., Friborg, T., Crill, P., Rakos, N., Kljun, N., Olsson, P.-O., Eklundh, L., Persson, A., and Rinne, J.: Field-scale CH₄ emission at a subarctic mire with heterogeneous permafrost thaw status, *Biogeosciences*, 18, 5811–5830, <https://doi.org/10.5194/bg-18-5811-2021>, 2021.